International
Collaboration
Center
Institute for Materials Research
Tohoku University
ICC-IMR

ICC-IMR FY2014
Activity Report

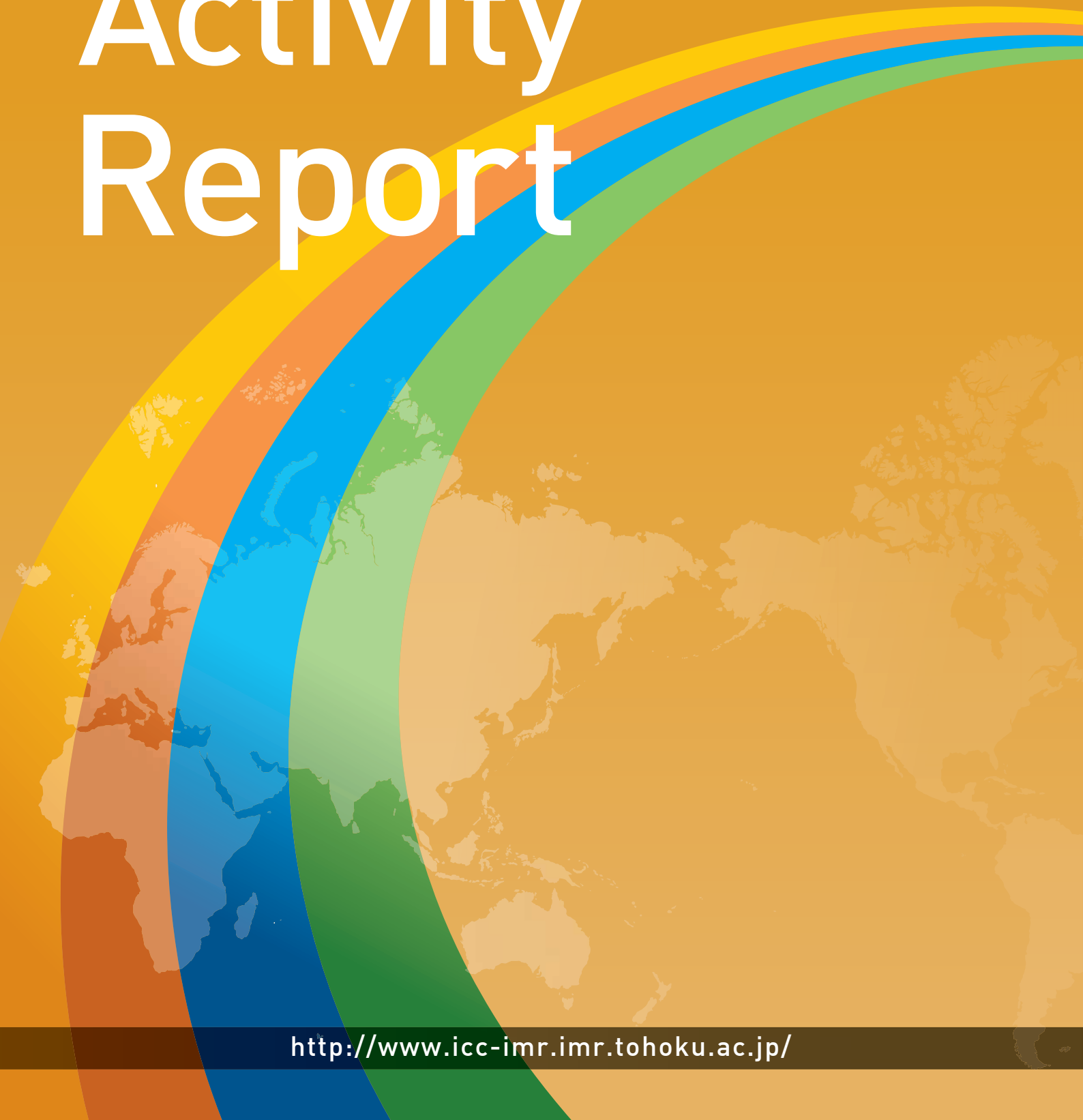

http://www.icc-imr.imr.tohoku.ac.jp/

ICC-IMR FY2014

Activity Report

International Collaboration Center

Institute for Materials Research
Tohoku University

CONTENTS

Mission

The ICC-IMR was founded in April 2008 as the center for international collaboration of the Institute for Materials Research (IMR) a center of excellence in material science, consisting of 27 research groups and five research centers. The ICC-IMR works as a gateway of diverse collaborations between overseas and IMR researchers. The ICC-IMR has invited 40 visiting professors and conducted 16 international research projects since its start-up (please inspect the graph below for more details,). The applications are open to foreign researchers and the projects are evaluated by a peer-review process involving international reviewers.

ICC-IMR coordinates six different programs:

1) International Integrated Project Research
2) Visiting Professorships
3) Short Single Research Visits
4) International Workshops
5) Fellowship for Young Researcher and PhD Student
6) Material Transfer Program

We welcome applicants from around the globe to submit proposals!

Visitors supported by ICC-Programs.

USA	67	Norway	4	Austria	1
China	48	Taiwan	4	Belgium	1
Germany	46	Italy	3	Czech Republic	1
Korea	42	Mexico	3	Denmark	1
France	37	Poland	3	Indonesia	1
UK	31	Singapore	3	Slovakia	1
Netherlands	17	Spain	3	Thailand	1
Russia	14	Australia	3	Turkey	1
India	7	Hong-Kong	2	Vietnam	1
Iran	6	Slovenia	2		
Switzerland	6	Ukraine	2		
Canada	4	Argentina	1		

ICC-IMR COMMITTEE MEMBERS

Director

Prof. Hiroyuki NOJIRI

Steering Committee

Prof. Shin-ichi ORIMO

Prof. Eiji SAITOH

Prof. Gerrit E. W. BAUER

Prof. Hitoshi MIYASAKA

Prof. Akira YOSHIKAWA

Assoc. Prof. Hidemi KATO

Activity Report

Visiting Scholars

FY 2014 Visiting Scholars

No.	Candidate	Host	Proposed Research	Title	Affiliation	Term
14G1	Siu-Tat Chui	G. Bauer	Spin Plasmonics	Professor	University of Delaware, USA	2014. 9.11- 12.10
14G2	Subhankar Bedanta	K. Takanashi	Magnetization Reversal Processes in Perpendicularly Magnetized FePt Dots and Antidot Arrays	Reader in Physics	National Institute of Science Education and Research (NISER), India	FY2014
14G3	Gunawarman Janawar Bin Janawa	M. Niinomi	Corrosion Behavior of New Beta Type Titanium Alloys in Modified Artificial Saliva	Professor	Andalas University, Indonesia	2014. 7.1- 8.31
14G4	Christian Wetzel	T. Matsuoka	Development of GaInN Heterostructures of High InN Fraction	Professor	Rensselaer Polytechnic Institute, USA	2014. 9.8-11.30
14G5	Masaaki Matsuda	M. Fujita	Neutron Scattering Study in Strongly Correlated Electron Systems	Senior Research Staff	Oak Ridge National Laboratory, USA	FY2014
14G6	Vladislav Kataev	H. Nojiri	Exploring the Phase Diagram of the Frustrated Quantum Spin Magnet $LiCuSbO_4$	Head of the Research Group	Leibniz Institute for Solid State and Materials Research IFW Dresden, Germany	2014.10.7-11.11

Spin Plasmonics

We demonstrated during this ICC-IMR project that the FMR absorption of a very thin insulating magnetic film can be enhanced by placing it on top of a dielectric. We find that the signal is enhanced by at least an order of magnitude due to a new nonreciprocal interface resonance that is a mixture of the magnetic surface plasmon mode and a wave-guide mode. Our model applies to experiments performed in the YIG/GGG system. Indeed, our picture resolves the disagreement on the magnitude of the spin diffusion lengths obtained with the FMR and the Brillouin scattering techniques. It also provides for a way to make new adaptive thin film miniaturized photonic nonreciprocal devices with low loss.

Spintronics with magnetic insulators exhibits less loss than spintronics with magnetic metals. To study spintronics with magnetic insulators, recent studies involve driving with external electromagnetic (EM) fields thin magnetic yttrium iron garnet ($Y_3Fe_5O_{12}$, YIG) films [1-3] with thicknesses of the order of nanometers. In metals, due to the eddy current, the signal is absorbed within a skin depth that is of the order of a micron. In insulators no currents can be generated, the signal is absorbed in a length scale of the order of a wavelength that is of the order of a cm. The ferromagnetic resonance (FMR) signal is much weakened when the film becomes very thin and it is important to find ways to increase the signal strength. Ever since the discovery of surface enhanced Raman scattering, much work has been done in the area of plasmonics in enhancing the absorption of EM fields on films with surface resonances. For magnetic systems, there is a corresponding analog of the ideas of plasmonics [4], which involves the magnetic surface plasmon (MSP) that is also known as the Damon Eshbach mode. The MSP comes from a coupling of the electromagnetic wave and the surface spin wave that produces a magnetic charge density, similar to the surface plasmon, which comes from a coupling of the electromagnetic wave and the electronic charge density. In this project we demonstrated how to enhance the absorption of EM waves for insulating magnetic films with spin plasmonics [4]. Motivated by ideas in plasmonics, we consider placing the film on top of a dielectric as shown in Fig. 1.

We found that the signal is enhanced by orders of magnitude due to a nonreciprocal interface resonance that is a mixture of the magnetic surface plasmon mode and a wave-guide mode. The line width of absorption is reduced by an order of magnitude less than the Gilbert damping parameter. At some frequency, the group velocity of this resonance is negative.

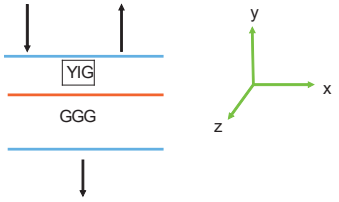

Fig.1: The geometry of the system and the wave vectors we have in mind. The coordinate system is also shown.

Experiments have been carried out in which very thin YIG films are grown on a gadolinium gallium garnet. ($Gd_3Ga_5O_{12}$, GGG) substrate. Theoretically, the substrate can be considered the dielectric.

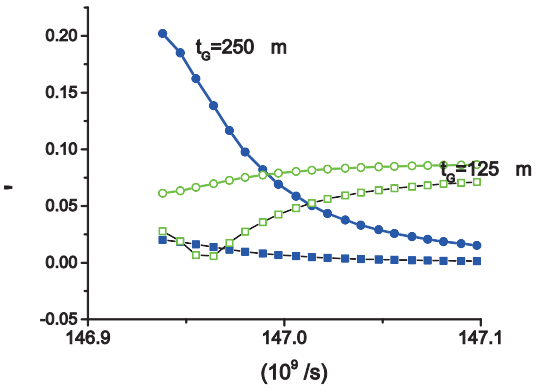

Fig.2: The normalized effective Gilbert damping parameter as a function of the angular frequency in units of 10 GHz. The thickness of the GGG is 250 micron (solid symbols) and 125 micron (open symbols). The larger damping curves are for the smaller wave vector resonances.

Keywords: ferromagnetic, insulator
Siu-Tat Chui (University of Delaware), E-mail: chui@bartol.udel.edu
http://www.bartol.udel.edu/~chui/

Recent experimental results of the damping of FMR [1,2] but not Brillouin scattering [3] can be interpreted in this light. Our theory provides for an explanation of the different results for the spin diffusion length obtained with the two experimental techniques. It also provides for a way to make new adaptive thin film miniaturized photonic nonreciprocal devices with low loss.

References

[1] C.W. Sandweg, Y. Kajiwara, A.V. Chumak, A. A. Serga, V. I. Vasyuchka,1 M. B. Jungfleisch, E. Saitoh, and B. Hillebrands, Phys. Rev. Lett. **106**, 216601 (2011).
[2] B. Heinrich *et al.*, Phys. Rev. Lett. 107, 066604 (2011); Appl. Phys. Lett. 100, 092403 (2012); H. Chang, P. Li, W. Zhang, T. Liu, A. Hoffmann, L. Deng, and M. Wu, IEEE Magn. Lett. **5**, 6700104 (2014).
[3] M. B. Jungfleisch, W.i Zhang, W. Jiang, H. Chang, J. Sklenar, S. M. Wu, J. E. Pearson, A. Bhattacharya, J. B. Ketterson, M. Wu, and A. Hoffmann, arXiv:1412.4032v1 and to appear in J. Appl. Phys. May, (2015).
[4] S. T. Chui, Z.-F. Lin, Chin. Phys. B **23** 117802. (2014); S. T. Chui, J. Appl. Phys. **117**, 183902 (2015).

Keywords: ferromagnetic, insulator
Siu-Tat Chui (University of Delaware), E-mail: chui@bartol.udel.edu
http://www.bartol.udel.edu/~chui/

Magnetization reversal processes in perpendicularly magnetized FePt dots and antidot arrays

We have fabricated FePt dot and antidot lattices with various diameters *d* ~ 40 nm, 100 nm, and 200 nm by electron beam lithography. The antidots were fabricated with square, circular and triangular shapes. Magnetization reversal in these FePt nanosized-arrays was studied by magneto-optical Kerr effect using the micro-sized laser spot. Magnetic force microscopy imaging revealed the reversal processes showing the domain wall trap in the antidote lattices.

The $L1_0$-FePt alloy is one of the most promising materials for future ultrahigh density magnetic storage devices because it possesses a huge uniaxial magnetocrystalline anisotropy (K_u = 7 x 10^7 erg/cc) which leads to the high thermal stability of magnetization in a nanometer scale. The aim of this international collaboration work is to understand the magnetization reversal processes in thin films, dots and antidots of FePt. In this collaboration, we first studied the magnetization reversal process in FePt thin films deposited on MgO (110) substrates exhibiting in-plane uniaxial magnetic anisotropy. The thin films were prepared by sputtering in the group of Prof. K. Takanashi, IMR, Tohoku University. It was found that the uniaixal magnetocrystalline anisotropy energy increased with the increase in film thickness and deposition temperature. Domain imaging performed by magneto-optic Kerr microscopy with a longitudinal geometry at NISER, India suggested that the domain structure and magnetization reversal process strongly depended on the film thickness and the deposition temperature. For the films deposited at a certain temperature, there exists a critical thickness where the coercive and saturation fields show maxima. [1]

Based on the experimental results for the FePt thin films, we investigated the details of magnetization reversal process for nano-structured FePt. Magnetic micro-/nano-structures are not only interesting for fundamental research but they have a high potential for applications. We studied on “negative” magnetic structure that was made using lithography to create a mesh of “holes” in a continuous FePt magnetic thin film. These negative structures are called as “antidots”. The array of such antidots is called as “magnetic antidot lattice (MAL)”. MALs are receiving intense research interest because of their potential advantages, such as lack of superparamagnetic limit to the bit size (as compared to dot arrays). The domain wall (DW) motion and their dynamics in such MAL system have not been studied so far. The major question is how a magnetic DW will behave in a MAL system where there are periodic defects. Also so far a systematic study on MAL systems for various shape, size and interdot spacing has not been performed. The domain nucleation, domain size and shape will certainly be affected by the shape and size of antidots. In this context, one goal of this collaboration work is to reveal the domain formation and measure the DW velocity as a function of applied magnetic fields with the Kerr microscopy.

It should be noted that magnetization reversal of the perpendicularly magnetized FePt antidots have never been studied. As the first step to reveal the DW dynamics in MALs, we focused on the magnetization reversal study of $L1_0$ ordered FePt antidot systems during my stay in IMR. We have fabricated MALs with the dimension of the antidots ranging from 200 nm to 40 nm. MAL arrays for various types of lattices such as square and honeycomb were fabricated in order to study the effect of the lattice pattern on the magnetization reversal. Scanning electron microscope (SEM) revealed that the size and shape of the antidot lattices were well controlled. Fig. 1 shows the SEM images of two representative FePt MALs on MgO (100) substrates.

Magnetic hysteresis loops were measured by a magneto-optical Kerr effect set-up using the micro-sized laser spot in the polar configuration, which revealed that coercivity in the antidot lattices strongly dependent on the size of the antidots (data not shown). In order to understand the domain structure we performed magnetic force microscope (MFM) observation under external fields. Fig. 2 shows the MFM images of an antidot lattice where the length of the antidots is 200 nm. It is noticed that domain walls are trapped between the antidot structures. Under external magnetic field the domains grow but their expansion is limited within the antidot structures. The observed MFM results are well reproduced by micromagnetic based OOMMF (Object oriented micromagnetic framework) simulations (data not shown). Kerr microscopy measurements are being investigated on the antidot samples in NISER, India.

In addition to the FePt antidots, we have performed the research work on magnetization reversal process in the perpendicularly magnetized FePt dots, and observed the “superferromagnetic behavior” in

the artificially fabricated structures [2].

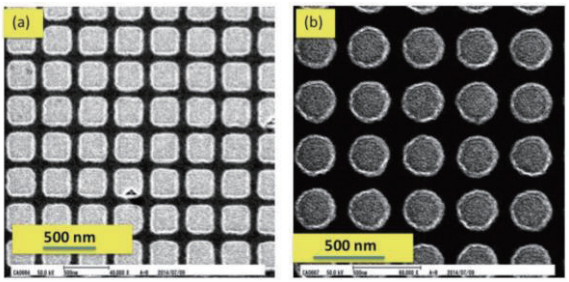

Fig. 1 Scanning electron microscopy images of FePt antidot lattices with (a) rectangular and (b) circular shapes of the holes.

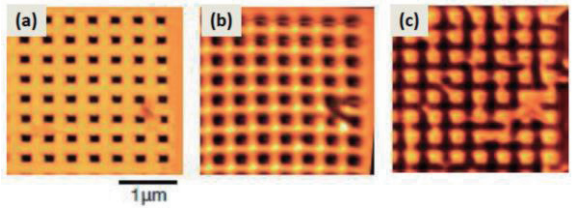

Fig. 2 (a) Morphology of a FePt antidote lattice with d = 200 nm. The image shown in (b) is the magnetic domain structure taken after remanence after positive saturation. (c) Magnetic domain image taken near coercive field of $\mu_0 H$ = -0.15 T.

References

[1] S. Mallick, S. Bedanta, T. Seki and K. Takanashi, J. Appl. Phys. **116**, 133904 (2014).

[2] S. Bedanta, T. Seki, H. Iwama, T. Shima, and K. Takanashi (to be published).

Keywords: magnetic, nanostructures, scanning electron microscoscopy
Full Name: Dr. Subhankar Bedanta, Reader in Physics, National Institute of Science Education and Research (NISER), Bhubaneswar, Odisha, India-751005
E-mail: sbedanta@niser.ac.in

Corrosion Behavior of New Beta Type Titanium Alloys in Modified Artificial Saliva

In order to know exactly the corrosion behavior of a new developed β type titanium alloy Ti-29Nb-13Ta-4.6Zr (TNTZ) in oral cavity environment, corrosion rate of this alloy in a modified artificial saliva was then investigated by using potensiostat in IMR. The corrosion rate of the most popular titanium, Ti-6Al-4V was also determined for comparison. Corrosion rate of TNTZ in the modified artificial saliva solution is much lower than that of Ti-6Al-4V due to formation of passive layers of Ti, Nb, Zr and Ta oxides in the surface of TNTZ.

It is reported that TNTZ alloy can have wide range of mechanical properties by performing heat treatment or thermo-mechanical treatments [1,2]. This alloy has an excellent corrosion resistance in air and body fluids [3-5]. In order to know the behavior of this alloy in oral cavity environment, corrosion rate of this alloy is then investigated in modified artificial saliva medium. Our previous investigation in Indonesia on the corrosion test of TNTZ in artificial saliva using weight loss method indicates that the weight loss of TNTZ is zero up to exposuring time of 480h [6]. At the same time, weight loss of two conventional alloys for dental application; stainless steel (SS) and cp-Ti can be easily measured, that is 0.01g and 0.03 g, respectively. In order to know exactly the corrosion rate of TNTZ in a modified artificial saliva, the corrosion rate is then measured by using potensiostat in IMR. The corrosion rate of the most popular titanium, Ti-6Al-4V was also determined for comparison.

The samples of TNTZ contains (in mass%) 31.5Nb, 11.6Ta, 4.7Zr, 0.03Fe, <0.02Al and bal. While, the content of Ti-6Al-4V (Ti64) is 6.2 Nb, 3.9V,87Ti and remains other elements. Three pieces of circular plate specimens of TNTZ and 3 pcs of those Ti64 with a diameter of 10 mm and 3 mm thickness were machined from as-received bars. All sample surfaces were grinded, polished and cleaned prior to corrosion test to obtain smooth surface specimens. The surface of specimens was then fully covered with epoxy resin except for top surface for exposing to the artificial saliva solution.

Corrosion measurements were conducted in 600ml solution of artificial saliva Fuyasama Meyer containing 0,4g NaCl, 0.4g KCl, 0.795g $CaCl_2.2H2O$, 0.69g NaH_2PO_4, and 1 g urea, maintained at pH 5.2 and 37°C using a potentiostat model (VERSA studio-200) controlled by a personal computer. Potentiodynamic polarization studies were carried out at a scan rate of 1 mV/s to obtain Tafel slot of all 6 specimens. After corrosion test, specimen surfaces were observed by SEM, EDX and XPS.

Tafel curve of all specimens that is obtained from potensiostat test is shown in Fig.1. While calculation result of the Tafel curve is tabulated in Table 1. It can be seen that I_{corr} of TNTZ is much smaller than that of Ti64. As for the average E_{corr} of TNTZ is also smaller that of Ti64. However, the E_{corr} of Ti64 is more stable than that of TNTZ. Since corrosion rate (CR) is proportional to I_{corr} value, the corrosion rate of TNTZ is much lower than that of Ti64. Averaged corrosion rate of TNTZ is $4{,}48 \times 10^{-9}$ *mmy*$^{-1}$, while Ti6Al4V is $6{,}37 \times 10^{-8}$ *mmy*$^{-1}$. This rate indicates that the corrosion rate of TNTZ is much smaller than the conventional dental wires of NiTi and stainless steel at pH 5 [7].

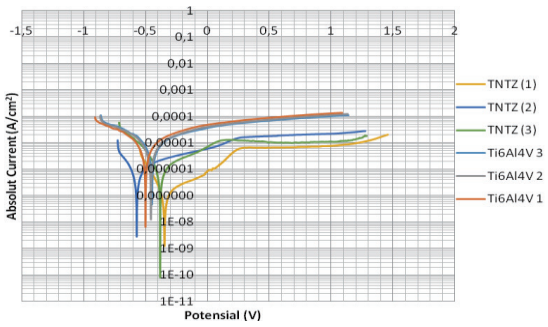

Fig. 1. Tafel plot TNTZ and Ti64 specimens

Table 1 Result of potensiostat test on TNTZ and Ti6Al4V

Specimen		I_{corr} (A)	E_{corr} (mV)	CR (mmy^{-1})
TNTZ	1	$1{,}57 \times 10^{-7}$	-350	$1{,}36 \times 10^{-9}$
	2	$6{,}99 \times 10^{-7}$	-570	$6{,}00 \times 10^{-9}$
	3	$6{,}91 \times 10^{-7}$	-380	$6{,}07 \times 10^{-9}$
	Avrg	$5{,}16 \times 10^{-7}$	-433	$4{,}48 \times 10^{-9}$
Ti-64	1	$7{,}29 \times 10^{-6}$	-406	$6{,}33 \times 10^{-8}$
	2	$7{,}51 \times 10^{-6}$	-440	$6{,}52 \times 10^{-8}$
	3	$7{,}20 \times 10^{-6}$	-490	$6{,}25 \times 10^{-8}$
	Avrg	$7{,}33 \times 10^{-6}$	-463	$6{,}37 \times 10^{-8}$

SEM observation shows that there is micro-pitting in TNTZ and Ti64 (Fig.2). Micro-pitting in TNTZ is deeper than that in Ti64. EDX examination near pitting area show that the content of oxygen in this area is much higher than other area on the surface of TNTZ (Fig.3). This confirms formation of pitting corrosion in this area. However, the pitting area of Ti64 is swallower than that of TNTZ.

Typical binding energy of TNTZ is shown in Fig. 4. This XPS result show that binding energy and intensity of Oxygen and Titanium is higher than that of Nb, Zr and Ta. The binding energy of those of Ti64. This indicates that formation of predominantly TiO_2 layer in the surface of TNTZ in addition to Nb, Zr and Ta oxides. While, binding energy and intensity of oxygen and Titanium in Ti64 is lower than those of TNTZ.

We need some discussion with Prof. Niinomi and his laboratory members to interprete this result. However, the limitation of time ask us to back to our country. It is great pleasure for me to join in Biomaterial Science for 2 months (July and August 2014). Thank you very much to Prof.Niinomi, Dr. Nakai and all IMR staff for kindness and cooperation during this visiting professorship.

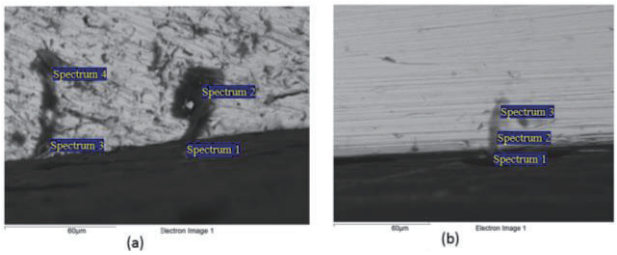

Fig.2 SEM micrograph of (a) TNTZ dan (b) Ti64

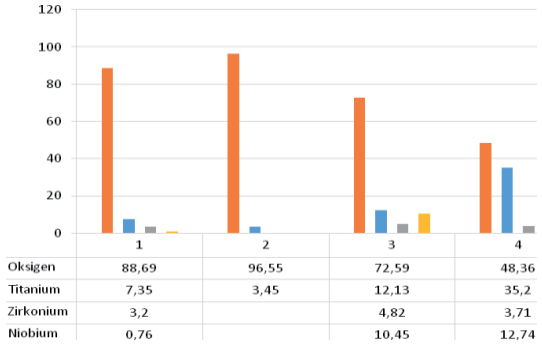

Fig.3 Element distribution near micropitting of TNZ

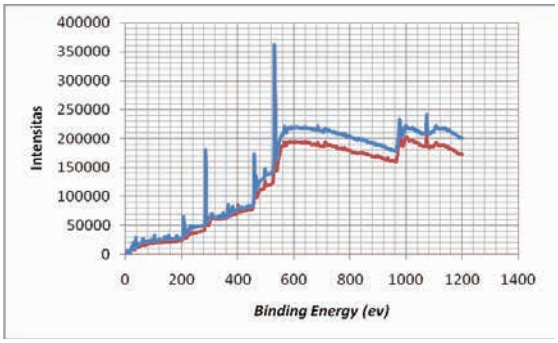

Fig.4. Binding energy spectrum of TNTZ

References

1. M . Niinomi, Mat. Mater. Trans. A 33A (2002) 477–486.
2. N. Sakaguchi, et al, H. Toda, Mater. Sci. Eng. C 25 (2005) 370.
3. T. Akahori et al, Materials Transactions, Vol. 45, No. 5 (2004) pp. 1540 to 1548
4. N. Diomidis, et al, Wear 271(2011) 1093–1102
5. M. Karthega, et al, Acta Biomaterialia 3 (2007) 1019–1023.
6. Gunawarman et al, Proc. of JSME chapter Indonesia Seminar, SNTTM XII, Jakarta 2012.
7. A. M. Barcelosa, et al. Materials Research. 16:1 (2013) 50-64.

Keywords: Corrosion, Biomedical
Gunawarman (Biomaterial Science Laboratory)
E-mail: gunawarman@ft.unand.ac.id
http://www.mesin.ft.unand.ac.id

Development of GaInN Heterostructures of High InN Fraction

After the development of red and blue LEDs, efficient emitters in the green spectral region are of prime relevance to energy-efficient solid-state lighting. Here GaInN layers of high InN-content are deemed key. Huge lattice-mismatch to GaN, however, likely renders such GaInN layers highly defective and strong piezoelectric fields reduce the radiative efficiency. Therefore, strategies are being devices that gradually reduce the mismatch between desired well-compositions and their embedding barrier layers.

First generation LED light sources rely on a blue emitting LED whose light is partially converted by a layer of phosphor to provide a broad spectrum akin to white light. For higher efficiency and better control of the spectrum, it should be better to combine the light of blue, green and red LEDs instead. Yet, there is a big variation of efficiency with wavelength. The concept of "green gap" nicely describes this shortcoming in the green and amber spectral regions. Here this is where we see tremendous improvement potential by advanced epitaxial processes for $Ga_{1-x}In_xN$ of high InN fractions *x*. We therefore work to improve the efficiency of such direct emitting LEDs in the longer wavelength green, amber and red spectral region.

One of the biggest challenges in this is the development GaInN epitaxial layers with low residual defect densities. So far it is commonly observed that the structural defect density of $Ga_{1-x}In_xN$ increases with InN fraction as needed for the longer wavelength emission.

LED devices grown on micro-patterned sapphire substrates have shown a 20% increase in light output power over unpatterned devices, and also showed a 20% increase in external quantum efficiency.[1] Moreover, even higher improvements were found when switching from patterning on the micrometer length scale to the patterning on the nanometer length scale, i.e. patterns sizes on the order of hundreds of nanometer.[2],[3],[4]

In this collaborative project we particularly explored the opportunity for fabrication of non-polar growth of a-plane GaInN/GaN heterostructures on r-plane sapphire substrates by MOVPE. An initial layer of a-plane GaN is grown on r-plane sapphire and demonstrates the usual high defect densities. After growth interruption, a 200 nm SiO_2 layer followed by a 10 – 40 nm layer of Ni was deposited. By rapid thermal annealing, Ni was transformed to self-assembled nano islands that then served as an etch mask for the underlying GaN. After RIE-ICP etching the template wafer is then regrown with $Ga_{1-x}In_xN$.

A scanning electron microscopy (SEM) image of the cross section and top surface of the resulting structure is shown in Figure 1. GaN pillars from the nano patterned template are seen in the highlighted area. The regrown material is visible above the pillars. This image

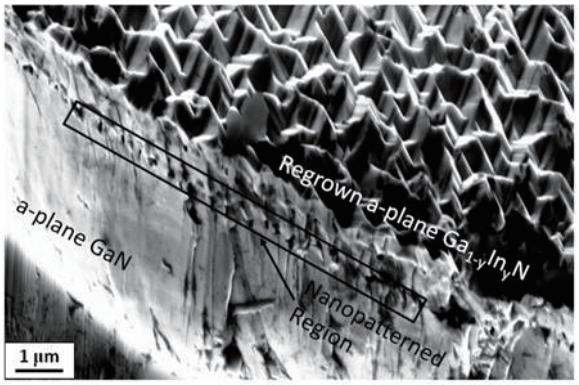

Figure 1 An SEM image showing the cleaved cross section and rough growth surface of this example of a-plane $Ga_{1-y}In_yN$ material grown on nano patterned a-plane GaN on sapphire.

reveals that a coalesced film was achieved, although the surface turns out to be quite rough. The roughness most likely is due to the low growth temperature as needed for high In-incorporation.[5]

Photoluminescence (PL) spectra were obtained before and after the $Ga_{1-x}In_xN$ regrowth as shown in Figure 2. The template shows the

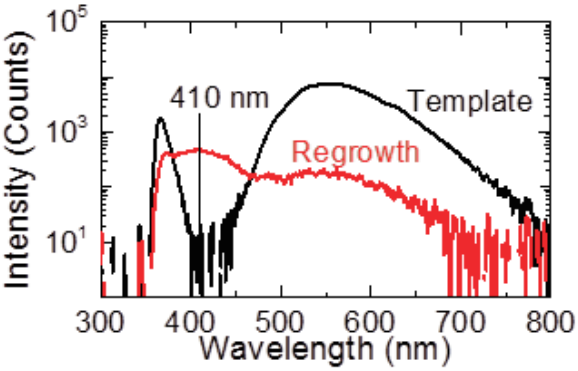

Figure 2 Photoluminescence spectra before and after a-plane $Ga_{1-x}In_xN$ regrowth.

near band-edge luminescence of GaN and the broad yellow luminescence. After regrowth of $Ga_{1-x}In_xN$, an additional contribution is seen near 410 nm, which should be attributed to the $Ga_{1-x}In_xN$ layers. Based on this peak wavelength, we estimate the InN content of some 3%. In x-ray diffraction, however, we have not been able to identify a separate relaxed layer of GaInN. This suggests that the regrown layer may have grown

pseudomorphically and could be under compressive stress.

In next steps we are now exploring paths to achieve a smoother surface texture, preferably on the nanometer roughness scale, and how to increase the incorporated InN fraction to the reach of 20% to 30%. A likely approach is the use of epitaxial growth along the negative c-axis of GaN which has shown promising aspects in the literature.[6]

References

[1] D. Wu, W. Wang, W. Shih, R. Horng, C. Lee, W. Lin and J. Fang, IEEE Photonics Technol. Lett., **17**(2), 288 (2005).

[2] Y. Li, S. You, M. Zhu, L. Zhao, W. Hou, T. Detchprohm, Y. Taniguchi, N. Tamura, S. Tanaka and C. Wetzel, Appl. Phys. Lett., **98**, 151102 (2011).

[3] C. Chiu, H. Yen, C. Chao, Z. Li, P. Yu, H. Kuo, T. Lu, S. Wang, K. Lau and S. Cheng, Appl. Phys. Lett., **93**, 081108 (2008).

[4] H. Huang, C. Lin, J. Huang, K. Lee, C. Lin, C. Yu, J. Tsai, R. Hsueh, H. Kuo and S. Wang, Materials Sci. Engin. B, **164**, 76 (2009).

[5] D. Koleske, S. Lee, M. Crawford, K. Cross, M. Coltrin and J. Kempisty, J. Crystal Growth, **391**, 85 (2014).

[6] T. Hirasaki, K. Asano, M. Banno, M. Ishikawa, F. Sakuma, H. Murakami, Y. Kumagai and A. Koukitu, Jpn. J. Appl. Phys., **53**, 05FL02 (2014).

Keywords: epitaxy, semiconducting, defects

Christian Wetzel (Rensselaer Polytechnic Institute)
E-mail: wetzel @rpi.edu
http://www.rpi.edu/~wetzel/

Development of Heusler crystals for neutron polarization analysis

Polarized neutron technique is indispensable for research in condensed matter physics. It is a powerful tool to separate nuclear and magnetic signals and determine detailed spin directions in the magnetic materials. We performed development of Heusler Cu_2MnAl crystals that will be used for polarizer on neutron spectrometers. We succeeded in finding optimum conditions to obtain high quality crystals with good polarization and high reflectivity.

Neutron has the spin degree of freedom (±1/2). Because of the interaction between the neutron spin and magnetic moments in materials, it is possible to separate nuclear and magnetic signals and also determine detailed spin directions in magnetic materials. Incident neutron beam should be polarized and the scattered beam's polarization should be analyzed to utilize these capabilities. There are several possibilities for the neutron polarizer and analyzer. Polarizing crystal, supermirror, and ^{3}He filter are widely used. Each device has merits and demerits, depending on instrument conditions, such as range of neutron energies and sample environments. Among these devises, we choose to use the crystal polarizer since it can be used with cryomagnet, the polarization property does not change with time, and it is almost free of maintenance.

Heusler Cu_2MnAl [1] is mostly used for the crystal polarizer because it shows reasonably good polarization and beam reflectivity or transmission. The crystal homogeneity and a slight amount of masaicity are essential to have good polarization and high reflectivity, respectively. However, commercially available crystals are sometimes not of high quality, although they are very expensive. In order to obtain high quality neutron polarizer (and analyzer), it is best to develop Heusler crystals in-house.

Institute for Material Research (IMR) at Tohoku University has the crystal growth and process facility. The Heusler crystals were grown and annealed at IMR. The crystal characterization was performed with neutron diffraction technique at High Flux Isotope Reactor (HFIR) at Oak Ridge National Laboratory (ORNL).

Heusler Cu_2MnAl crystals were grown using the Bridgeman method. Since the (111) reflection, which is a mixture of nuclear and magnetic reflections, is used to polarize and analyze neutron beam, the crystals are cut parallel to the (111) plane. Neutron beam is ideal to characterize the crystals because it can measure the bulk properties and directly measure polarization and reflectivity. The neutron scattering diffraction measurements were performed on the sample alignment instrument CG-1B and the polarized triple-axis spectrometer HB-1 at HFIR, ORNL.

Figure 1 shows a picture of typical crystals of Heusler Cu_2MnAl, which we used to characterize the crystal quality. The dimensions of the crystals are about 20 X 20 X 5 mm^3, in which the wide and flat plane is the (111) plane.

Figure 2(a) shows a rocking curve scan of the (111) Bragg peak in an as-grown crystal. We measured several crystals to check the sample dependence. Many of the as-grown crystals are found to show multi-grain structure and/or broad masaicity. The peak intensities are also similar when normalized by the crystal area. We also measured the reflectivity of the crystals. The reflectivity was estimated to be ~20%, excluding

Fig. 1 Typical Heusler Cu_2MnAl crystals used in this study. The flat plane is the (111) plane.

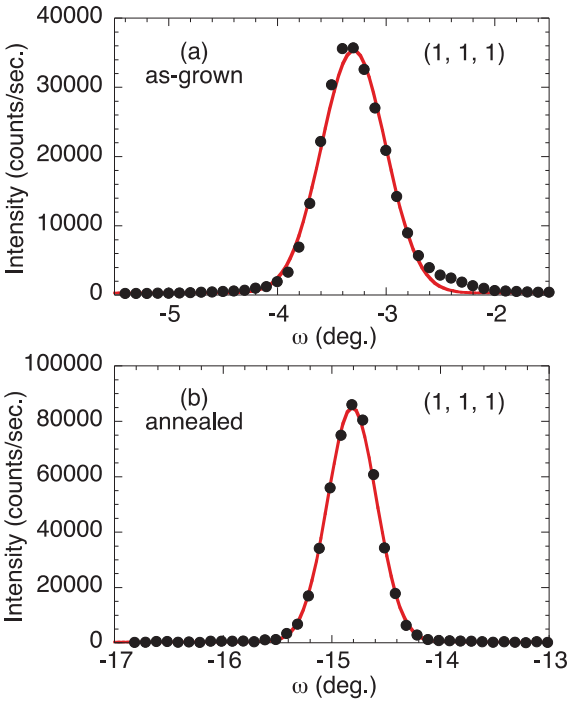

Fig. 2 Rocking curve scans of the (111) Bragg reflection in as-grown (a) and annealed crystals (b) of Heusler Cu_2MnAl. The measurements were performed using unpolarized neutrons. The solid lines are the results of fits to a Gaussian function.

the 1/2 polarization factor. This value is far below the required one (> 35%). The degree of order between Mn and Al is an important factor to realize good polarization. This can be estimated from the intensity ratio between the (111) and (222) Bragg peak intensities. R [=I(222)/I(111)] is about 2 for many of the crystals, indicating that the Mn and Al are well ordered and good polarization is expected.

Figure 2(b) shows a rocking curve scan of the (111) Bragg peak in an annealed crystal from the same lot, which the as-grown crystal is cut from. It is clear that the annealed sample shows stronger intensity and narrower mosaic (~0.5°) with single grain structure. The enhanced intensity by a factor of 2 implies that the reflectivity is improved to above 40%. The mosaic of 0.5° is ideal for polarizing monochromator and analyzer. R is calculated to be about 2, which is the same as that in the as-grown crystals.

The flipping ratios of the annealed crystals were also measured and found to be above 20 at a neutron energy of 13.5 meV, which corresponds to ~90% of polarization and is suitable for the neutron polarizer and analyzer. We also measured polarization of the crystals annealed with different conditions. The polarization is good for many of the annealed crystals. However, the reflectivity depends significantly on the annealing conditions. The highest reflectivity so far has been obtained with annealing at 600 °C for 4 hours and at 860 °C for 2 hours, then quench to room temperature. The post annealing makes the good reflectivity and less grain structure possible, although the polarization is already good in as-grown crystals.

Using these high quality crystals, we are first planning to make a neutron polarizing analyzer for the triple-axis spectrometer HB-1, which is more compact than the polarizing monochromator and easier to design. In order to enhance the scattering signal, the polarizer should have vertically focusing mechanism with the crystals magnetized vertically. As the next stage, we also plan to make the polarizing monochromator. Since high neutron beam flux is available on HB-1, more efficient and high quality polarization analysis will be feasible in the near future. This capability will enhance the research in strongly correlated electron systems, including high-T_c superconductors and multiferroic materials.

In summary, we succeeded in finding optimum conditions to obtain high quality Heusler Cu_2MnAl crystals with good polarization and high reflectivity. We plan to make neutron polarizing monochromator and analyzer, which have vertically beam focusing mechanism, for more efficient and high quality neutron polarization analysis.

This work was performed in collaboration with Y. Yamaguchi, K. Sato, K. Suzuki, M. Fujita (IMR), and H. Hiraka (KEK). This research at ORNL's High Flux Isotope Reactor was sponsored by the Scientific User Facilities Division, Office of Basic Energy Sciences, US Department of Energy.

References

[1] A. Delapalme and J. Scweizer, Nucl. Instr. Methods 95, 589 (1971).

Keywords: neutron scattering, crystal growth, magnetic
Masaaki Matsuda (Quantum Condensed Matter Division, Oak Ridge National Laboratory)
E-mail: matsudam@ornl.gov
http://neutrons.ornl.gov/ptax

Probing the phase diagram of the frustrated quantum spin magnet $LiCuSbO_4$ with high-field ESR spectroscopy

The complex oxide $LiCuSbO_4$ has been recently put forward as a possible realization of the Heisenberg quantum spin-1/2 chain magnet which exhibits the so-called spin liquid state. During my research visit at the Institute for Materials Research we have undertaken a detailed study of this compound by high magnetic field ESR spectroscopy. The experimental data reveal interesting signatures of the conjectured magnetic field induced spin phase which possibly arises in this system at low temperatures close to the spin saturation field of 12 T.

Transition metal oxides provide indispensable playground for studies of fundamental models of quantum magnetism. Recently the $LiCuSbO_4$ (LCSO) was suggested as a material where a quantum spin-liquid state is possibly realized [1]. In LCSO the Cu^{2+} spins-1/2 are arranged in chains (Fig. 1) which are frustrated due to competing exchange interactions. Thermodynamics and neutron scattering data reported in Ref. [1] reveal short-range incommensurate spin correlations below $T \sim 8$ K. However, no long-range magnetic order was found down to 100 mK. The analysis of the dispersion of magnetic excitations has revealed the ferromagnetic nearest neighbor magnetic coupling $J_1 = -75$ K and a substantial antiferromagnetic next nearest neighbor coupling $J_2 = 34$ K. The ratio $|J_2/J_1| = 0.45$ exceeds the critical value of 0.25 that separates a collinear spin arrangement in the Heisenberg spin-1/2 chain for $|J_2/J_1| < 0.25$ from an incommensurate spin spiral configuration for $|J_2/J_1| > 0.25$. Interestingly, specific heat measurements suggest the occurrence of a magnetic field induced phase at $T < 2$ K close to the saturation field $B_s = 12$ T. Recent theories predict that close to B_s exotic spin-nematic (multipolar) order can occur in frustrated spin chains (see, e.g., [2]).

Using the excellent pulse magnetic field high-frequency electron spin resonance (ESR) facility at the IMR Tohoku we have studied a polycrystalline sample of LCSO in a broad range of excitation frequencies in the sub-THz domain, in magnetic fields up to 20 T and temperatures down to 500 mK.

At $T > 50$ K the ESR spectrum of LCSO at all studied frequencies exhibits a single line with the g-factor $g = 2.18$ typical for Cu^{2+}. At fields $B < 7$ T the signal remains single line and practically unchanged even at low temperatures (Fig. 2, left). In particular, no signatures of magnetic order could be revealed. However, a peculiar effect has been observed in the high field domain $B \geq 9$ T. There, below $T \sim 20$ K, the ESR spectrum develops a structure (Fig. 2, right). Besides the main peak P2, the low-field (P1) and the high-field (P3) satellites begin to develop. Their distance from the central peak P2 seems to be independent of the field strength but their intensity grows with field and with decreasing the temperature.

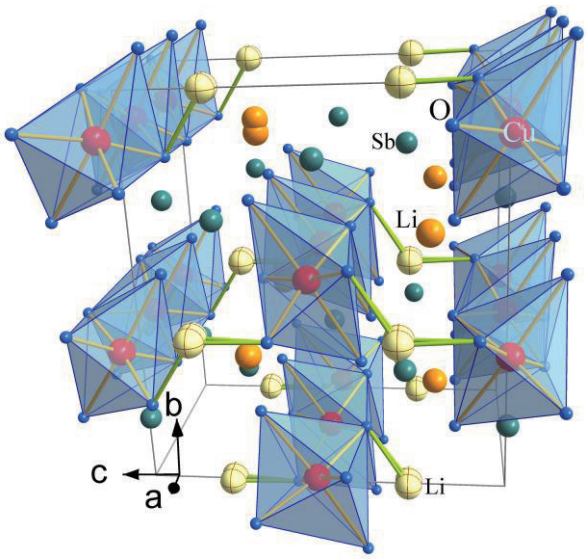

Fig. 1 Crystallographic structure of $LiCuSbO_4$. Cu^{2+} ions (red) bonded to O^{2-} ligands (blue) form edge-sharing CuO_6 chains along the a-axis and provide a realization of the one-dimensional Heisenberg spin-1/2 quantum magnet.

The structure in the ESR spectrum of LCSO is most likely not due to the g-factor anisotropy because it is absent at high temperatures despite the narrowing of the line at high T. It can be tentatively attributed to the growth of the short-range spin correlations in the low temperature regime. It is tempting to conclude that a possible reason for a peculiar shape of the ESR spectrum could be the development of a staggered field in the short-range ordered state. It is remarkable that the satellite peaks are seen only at high fields where the distinct

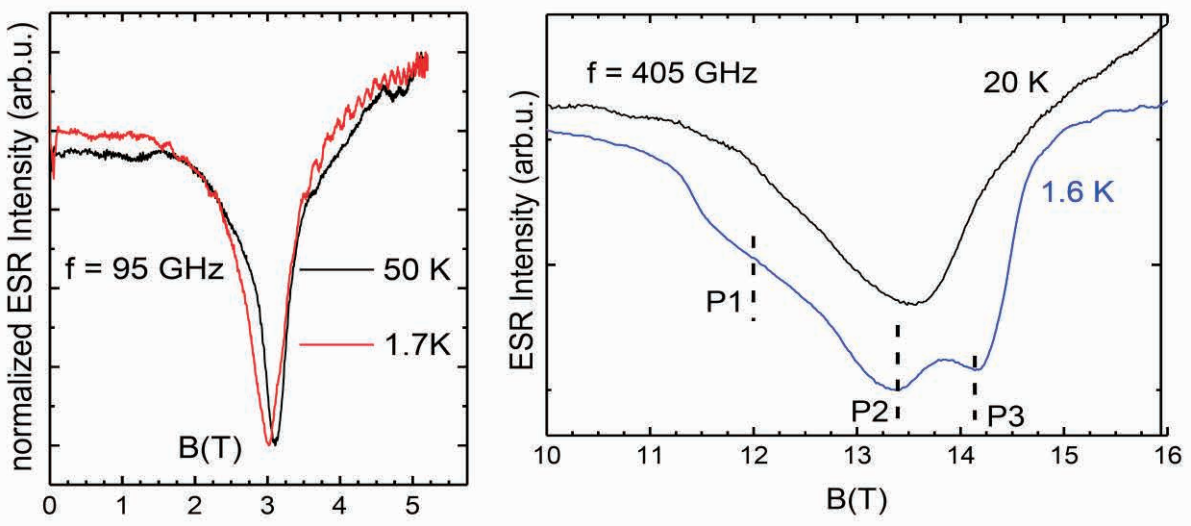

Fig. 2 Representative ESR spectra of $LiCuSbO_4$ at a frequency f = 95 GHz, and a resonant field B_{res} = 3 T (left), and at f = 405 GHz, B_{res} = 13.4 T (right). The spectrum remains single line down to low temperature at fields B_{res} < 7 T, but develops a structure (peaks P1, P2 and P3) at T < 20 K at higher fields

high-field phase has been identified near the saturation field B_S [1]. Motivated by this conjecture we have started a theoretical analysis of the possible spin structure of such high-field phase in LCSO. This work is currently in progress.

I am grateful to Prof. Hiroyuki Nojiri for a generous support of this project and his warm hospitality during my stay at the IMR.

References

[1] Dutton et al., Phys.Rev.Lett. **108**,187206(2012)
[2] M. Sato et al., Phys.Rev.Lett.**110**, 077206 (2013)

Keywords: magnetic properties; high magnetic field
Vladislav Kataev (Leibniz Institute for Solid State and Materials Research IFW Dresden)
E-mail: v.kataev@ifw-dresden.de
http://www.ifw-dresden.de/about-us/people/dr-vladislav-kataev/

Activity Report

Integrated Projects

FY2013-2014 Integrated Projects

No.	PI	Host	Proposed Research	Title	Affiliation	Term
13PJT1	Rodolphe Clérac	H. Miyasaka	New Approaches for Single-Chain Magnets and Related Magnetically-Correlated Materials	Researcher	Centre de Recherche Paul Pascal (CRPP), CNRS, France	FY2013-14
13PJT2	Sebastian Gönnenwein	G. Bauer	Spin, Lattice, and Ac-Field Coupling in Magnetic Materials and Devices	Research Scientist	Walther-Meissner-Institute, Bavarian Academy of Science, Germany	FY2013-14
13PJT3	Björn C. Hauback	S. Orimo	New Guideline for Designing Hydrogen Storage Complex Hydrides	Head of Department	Physics Department, Institute for Energy Technology, Norway	FY2013-14
13PJT4	Georg Knebel	D. Aoki	High Pressure Studies of Strongly Correlated Electron Systems	Researcher	SPSMS, UMR-E CEA, France	FY2013-15
13PJT5	Darren Graham	H. Nojiri	New Technology for Materials Science: Developing a Terahertz-Frequency EPR Spectrometer	EPSRC Research Fellow and Lecturer of Physics	Photon Science Institute and School of Physics and Astronomy, The University of Manchester, UK	FY2013-14

New Approaches for Single-Chain Magnets and Related Magnetically Correlated Materials

In order to reveal new theories or new techniques for capturing magnetic dynamics or spin transition in metal-complex-based compounds, we focused here on two types of magnetic compounds, (I) a family of alternating chain compounds composed of Mn^{III} salen-type complexes and TCNQ derivatives ($salen^{2-}$ = N,N'-ethylenebis(salicylideneiminate); TCNQ = tetracyano-p-quinodimethane), which is a target for Single-Chain Magnets with a strong correlation beyond the Ising limit, and (II) a family of cyano-bridged Co^{II}-Fe^{III} dinuclear compounds that occur an electron transfer at around 100 K to be a Co^{III}-Fe^{II} oxidation state at lower temperatures with accompanying a spin transition between high spin at the high temperature region and low spin at low temperature region in different structural space groups, respectively.

The researches on "molecular quantum magnets" that exhibit slow relaxation of the magnetization such as Single-Molecule Magnets (SMMs) have been carried out energetically in the wide fields of chemistry and physics since the beginning of 1990s, and some applications for nanotechnology have been tried in recent years. In this class of materials, one-dimensional materials named Single-Chain Magnets (SCMs) are unique because slow dynamics of their magnetization is closely related to short-range correlations between anisotropic spin units (such as Ising-type spins) along the chain. Clérac and Miyasaka discovered this magnetic property for the first time in a ferromagnetically coupled Ising-like spin chain and they named this class of material as "Single-Chain Magnet" [1]. In comparison to SMMs, SCMs possess an additional degree of freedom than the magnetic anisotropy D of the chain spin unit (D defined by: $H = DS_z^2$): the exchange intra-chain coupling J (defined by: $H = -2J\Sigma S_i \cdot S_{i+1}$) [2]. This parameter is a real advantage as it can be controlled by an external stimuli, for example by light irradiation, and thus, the SCM behavior could be finely tuned. In addition, we revealed that the SCM behavior might also be affected by a third degree of freedom, i.e. the inter-chain antiferromagnetic interactions J' [3,4]. Thus, we realize that intra-chain and inter-chain exchange couplings are more flexible and tunable parameters in this type of magnetic materials compared to the magnetic anisotropy, and this type of one-dimensional systems appears to be a good platform to observe boundaries between quantum and bulk (continuum) regimes. Furthermore, recently, we revealed that the SCM behavior is observed not only in the Ising limit with $|D/J| >> 4/3$, but also in other limits like $|D/J| \leq 4/3$ in the case where J is relatively large [5,6]. In such systems, the understanding of the domain walls is a key to understand their dynamic behavior. These results indicate that such one-dimensional magnetic materials can potentially be modulated at the molecular level

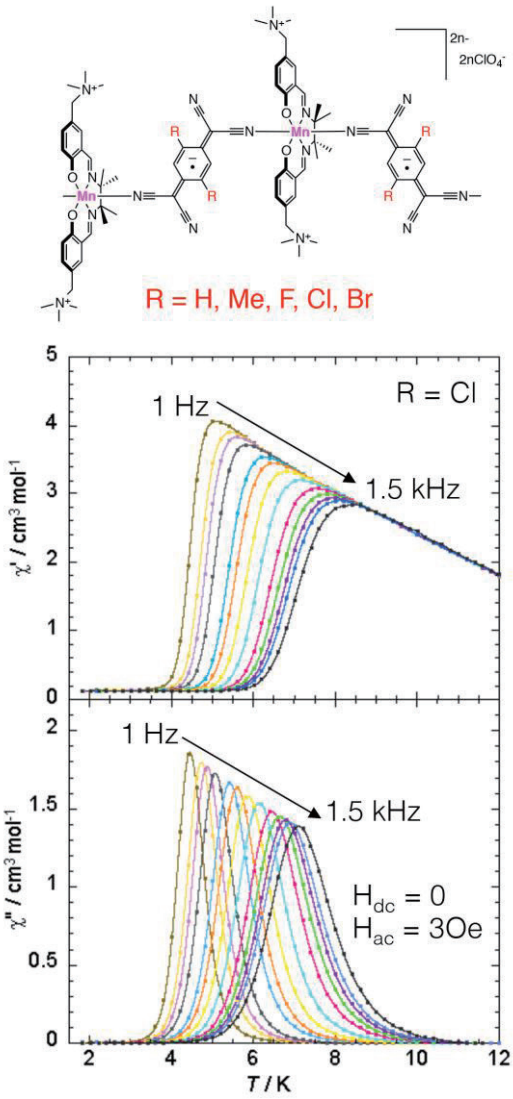

Fig. 1 A schematic representation of the target compounds in the project (I), which are SCM chains composed of Mn^{III} salen-type complexes and TCNQ derivatives, and the temperature dependence of ac susceptibilities (χ': in-phase; χ'': out-of-phase) for the R = Cl compound.

by multiple degrees of freedom giving the opportunity of design the next generation of magnets.

Here, we, in particular, focused on two target materials: (I) SCMs with strong correlations in |D/J| < 4/3, and (II) heterometal compounds that occur a temperature-dependent inter-metal electron transfer. The latter target is not for SCM, but providing a new spin-switching system useful even for SCM works in future.

In the work on the target material (I), we designed a family of alternating chain compounds composed of Mn^{III} salen-type complexes ($salen^{2-}$ = N,N′-ethylenebis(salicylideneiminate)) and TCNQ derivatives (TCNQ = tetracyano-p-quinodimethane; $TCNQR_x$ = $TCNQF_2$, $TCNQCl_2$, $TCNQBr_2$, $TCNQMe_2$ as already synthesized for the original TCNQ unit (Fig. 1) [5]. These compounds have similar chain forms, but provide different exchange coupling constants, even though all are adopted in the relation of the |D/J| < 4/3. All compounds exhibited similar spin dynamics behavior as SCMs (Fig. 1) [5], but not followed in the theory of Glauber dynamics for |D/J| >> 4/3. Thus, this dynamics behavior could be due to the motion of domain wall, which should be explained using a different theory from the Glauber dynamics [7].

In the work on the target material (II), the French team of Dr. R. Clérac (CRPP, CNRS, France) and Prof. C. Mathoniere (Université Bordeaux 1/ICMCB, France) prepared materials of cyano-bridged Co^{II}-Fe^{III} dinuclear compounds with different counter anions (Fig. 2). This family of paramagnetic compounds exhibited temperature-dependent inter-metal electron transfer to cause a Co^{III}-Fe^{II} low spin system that was diamagnetic. Interestingly, this transition involved a structural modification changing its space group from Pnma for the high temperature region (paramagnetic) to $P2_12_12_1$ for the low temperature region (diamagnetic) in the orthorhombic system. Thus, this transition was confirmed by temperature dependence of magnetic properties, which occur a spin transition from a paramagnetic state with S = 3/2 to a diamagnetic state at the transition temperature, and structures measured at higher/lower temperatures than the transition temperature. Furthermore, the measurement of the permittivity of compounds in a pellet sample captured the transition in detail. These data proved that the electron transfer followed by a high spin/low spin transition simultaneously occurred with a reversible structural transition.

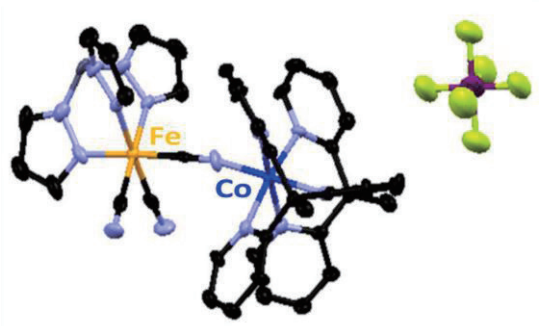

Fig. 2 Structure of cyano-bridged Fe^{III}-Co^{II} dimer, $[(Tp)Fe^{III}(CN)_3Co^{II}(PY5Me_2)]PF_6 \cdot 2DMF$, where the counter anion PF_6^- can be replaced by AsF_6^-.

References

[1] R. Clérac, H. Miyasaka, M. Yamashita and C. Coulon, J. Am. Chem. Soc. 124, 12837 (2002).
[2] C. Coulon, H. Miyasaka and R. Clérac, Struct. Bond. 122, 163 (2006).
[3] C. Coulon, R. Clérac, W. Wernsdorfer, T. Colin and H. Miyasaka, Phys. Rev. Lett. 102, 167204 (2009).
[4] H. Miyasaka, K. Takayama, A. Saitoh, S. Furukawa, M. Yamashita and R. Clérac, Chem. Eur. J. 16, 3656 (2010).
[5] H. Miyasaka, T. Madanbashi, K. Sugimoto, Y. Nakazawa, W. Wernsdorfer, K. Sugiura, M. Yamashita, C. Coulon and R. Clérac, Chem. Eur. J. 12, 7028 (2006).
[6] H. Miyasaka, T. Madanbashi, A. Saitoh, N. Motokawa, R. Ishikawa, M. Yamashita, S. Bahr, W. Wernsdorfer and R. Clérac, Chem. Eur. J. 18, 3942 (2012).
[7] O. V. Billoni, V. Pianet, D. Pescia and A. Vindigni, Phys. Rev. B 84, 064415 (2011).

Keywords: magnetic properties, spin transfer, dielectric properties
Hitoshi Miyasaka (Solid-State Metal-Complex Chemistry Division)
E-mail: miyasaka@imr.tohoku.ac.jp
http://www.miyasaka-lab.imr.tohoku.ac.jp/

Spin, lattice, and ac-field couplings in magnetic materials and devices

In this project, we studied new developments in spintronics related to the coupling between spins and magnetic order parameter with other degrees of freedom, specifically mechanical and electromagnetic fields. The present collaboration was carried out with contributions from the IMR experimental groups Saitoh and Takanashi and many theoretical and experiment groups from oversea, most importantly the Walter Meissner Institute of the Technical University Munich and the Kavli Institute of NanoScience of the Technical University Delft.

In this project, we studied many different phenomena, of which we present here three highlights, *viz*. the progress of our understanding the coupling with phononic and electromagnetic fields.

Spin Mechanics

The magnetization order parameter couples to the lattice by magnetic form and crystal anisotropies. In the past we investigated the effects of the coupled motion of the magnetic and the elastic fields for rigid systems. The other extreme, the magnon-phonon interaction in bulk ferromagnets, has been studied intensively many decades ago. Several modern developments, such as the ultrasound induced spin pumping discovered at the IMR, requires the development of new theoretical techniques. We developed a scattering theory for ultrasound actuation of magnetization dynamics [1]. By the spin pumping technique it should be possible to detect strongly coupled quasiparticle, the “magnon-polarons” as demonstrated in Fig. 1.

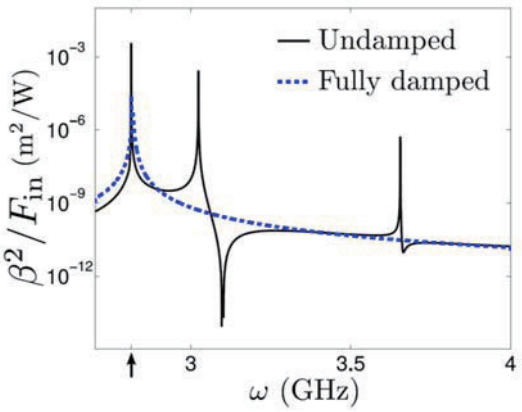

Fig. 1: *Normalized acoustically actuated spin pumping signal as function of the sound frequency for thin magnetic films (dashed line: thick films) [1].*

Strong coupling of microwaves with magnetic order parameter

We formulated a scattering theory to study magnetic films in microwave cavities beyond the independent-spin and rotating-wave approximations of the Tavis-Cummings model that is based on the coupled LLG and Maxwell equations [2]. When the coupling between spin and microwaves becomes larger than the losses of the cavity and by Gilbert damping, magnons and photons become indistinguishable and form new quasi-particles, so-called “magnon-polaritons”. We demonstrate that strong coupling can be achieved not only for the ferromagnetic resonance mode, but also for spin-wave resonances; the coupling strengths are mode dependent, as demonstrated in Fig. 2, and decrease with increasing mode index. The strong-coupling regime can be accessed electrically by spin pumping into a metal contact.

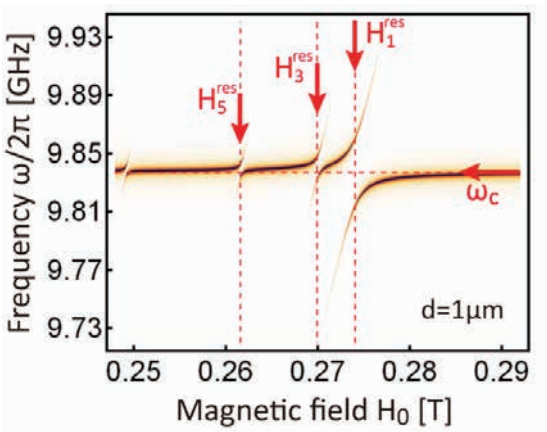

Fig. 2: *Microwave reflection generated by a magnetic film in a cavity, illustrating strong coupling of spin waves with the ac magnetic field [2].*

Strong coupling of microwaves with magnetic order parameter

T. Chiba *et al*. [3] predicted that the current-induced magnetization dynamics in magnetic insulators can be measured by down-conversion of an ac voltage in Pt contacts. The theory was based on the recently discovered spin Hall magnetoresistance (SMR) [4] and tested by the Munich group to unequally prove the actuation of the magnetic order parameter by the spin transfer torque [5].

Experiments were carried out in yttrium iron garnet/ platinum bilayers. An alternating charge current at GHz frequencies in the platinum gives rise to DC spin pumping and spin Hall

magnetoresistance rectification voltages, induced by the Oersted fields of the AC current and the spin Hall effect-mediated spin transfer torque. In ultrathin, yttrium iron garnet films, we observed spin transfer torque actuated magnetization dynamics that can be significantly larger than those generated by the AC Oersted magnetic field. The different effects can be shown to dominate for samples with different thicknesses as illustrated in Fig. 3, which compares experiments and theoretical modelling [3] Spin transfer torques thus efficiently couple charge currents and magnetization dynamics also in magnetic insulators, enabling charge current-based interfacing of magnetic insulators with microwave devices.

References

[1] A. Kamra, H. Keshtgar, P. Yan, G. E. W. Bauer, *Coherent elastic excitation of spin waves*, Phys. Rev. B **91**, 104409 (2015).

[2] Y. Cao, P. Yan, H. Huebl, S. T.B. Goennenwein, G.E.W. Bauer, *Exchange Magnon-polaritons in Microwave Cavities*, Phys. Rev. B **91**, 094423 (2015).

[3] T. Chiba, G. E. W. Bauer, S. Takahashi, *Current-induced spin torque resonance for magnetic insulators*, Phys. Rev. Applied 2, 034003 (2014)

[4] H. Nakayama, M. Althammer, Y.-T. Chen, K. Uchida, Y. Kajiwara, D. Kikuchi, T. Ohtani, S. Geprägs, M. Opel, S. Takahashi, R. Gross, G. E. W. Bauer, S. T. B. Goennenwein, and E. Saitoh, *Spin Hall Magnetoresistance Induced by a Nonequilibrium Proximity Effect*, Phys. Rev. Lett. **110**, 206601 (2013).

[5] M. Schreier, T. Chiba, A. Niedermayr, J. Lotze, H. Huebl, St. Geprägs, S. Takahashi, G. E. W. Bauer, R. Gross, S. T. B. Goennenwein, *Current-induced spin torque resonance of a magnetic insulator*, arXiv:1412.7460.

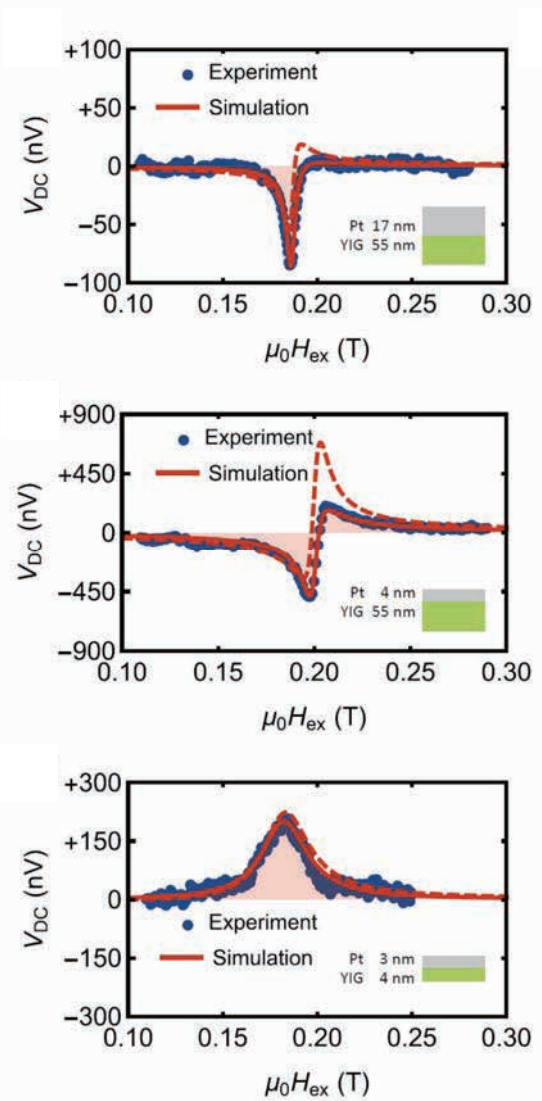

Fig. 3: *Measured (dots) and simulated (lines) of the dc voltage generated under and ac applied current for three different YIG|Pt samples with thicknesses indicated in the insets [5]. The dashed lines correspond to zero phase shift between the Oersted magnetic fields and the applied current.*

Keywords: magnetoresistance (transport), spin current
Gerrit E.W. Bauer (Theory of Solid State Physics, Institute for Materials Research, Tohoku University)
E-mail: ・・・・g.e.w.bauer@imr.tohoku.ac.jp
http://www.imr.tohoku.ac.jp/en/org/research/01.html

New guideline for designing hydrogen storage complex hydrides

Complex hydrides have potentials to store high hydrogen gravimetric and volumetric densities. In this project we have investigated crystal structures of complex hydrides for better understanding of the hydrogen storage properties at atomic level, and firstly proposed a crystal structural indicator for the hydrides. The indicator suggests a suitable crystal structure model and a criterion for the formation of the hydrides with specific anions.

Complex hydrides, which are composed of metal cations such as Li^+ and a homoleptic hydride complex such as $[AlH_4]^-$, have attractive material properties, such as the ability to be used in hydrogen storage, fast ionic conductivity, superconductivity and so on.

In particular, studies for developing of hydrogen storage materials on complex hydrides with high hydrogen gravimetric and volumetric densities have been intensively investigated since discovery of reversible hydrogen uptake and release reactions on Ti-enhanced $NaAlH_4$.[1, 2, 3] To date, we have found a linear relationship between the electronegativity of metal cations and thermodynamic stability related to hydrogen desorption temperature in complex hydrides.[4] The correlation has been widely acknowledged as a guideline for designing hydrogen storage complex hydrides. The results are expected to be true in isomorphic complex hydrides.

In addition to the correlation, it is challenging to understand the relationships between the material properties and the crystal structures with complicated atomic arrangements due to flexibility of the chemical bonds formed by hydrogen,[5] which are often difficult to determine. For instance, H^- and homoleptic hydride complexes such as pentagonal-bipyramidal $[CrH_7]^{6-}$ often coexist in complex hydrides.[6]

On the other hand, perovskite-type compounds have been acknowledged to be summarized by Goldschmidt tolerance factor, which has been frequently used to understand materials properties viewed from crystal structure in fundamental and applied studies, including material designs. Though the Goldschmidt tolerance factor has been used to study hydrides, it cannot be applied to materials that do not have perovskite-type structures. Thus different approaches are required to be able to study other hydride crystal structures. The availability of an appropriate approach could allow our understanding of the material properties associated with the presence of hydrogen in materials to be improved.

In this project, we focused on experimental and theoretical studies on crystal structures of complex hydrides.[5–10] From this project, we have successfully constructed an indicator (Fig. 1) for the crystal structures of Al-based complex hydrides, which are composed of metal cations and $[AlH_4]^-$ (tetra-alanates) or $[AlH_6]^{3-}$ (hexa-alanates).[10]

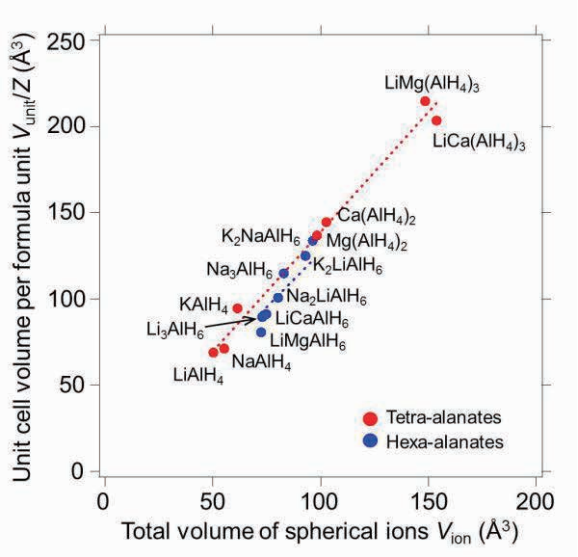

Fig. 1 Plots of V_{unit}/Z as a function of V_{ion}. Red and blue circles and dotted lines are plots and IFF for tetra-alanates and hexa-alanates, respectively.

The indicator is summarized by two types of volume: the unit cell volume (V_{unit}) normalized by the number of formula units (Z), V_{unit}/Z, and the total volume of the spherical ion, V_{ion}, of constituting the hydrides. These volumes allow the ionic filling fraction (IFF) of the hydrides to be determined. Interestingly, related hydrides with arbitrarily arranged ionic components including other complex hydrides can be also summarized by the same method. Then, the IFF followed a linear trend dependent on the type of hydride, and it could be used as a criterion for the formation of the hydrides with specific anions. The linearity of the IFF means that the initial crystal structure model, with a suitable unit cell and chemical formula, can be predicted. Based on the

indicator, we could determine the new crystal structures of the mixed metal cation complex hydrides $LiCa(AlH_4)_3$ and $LiCaAlH_6$ (Fig. 2).[10] In addition, we also suggest that the use of the indicator can be extended to other ionic compounds, including halides and oxides, for which we identify similar trends to those found for the hydrides. Our approach could therefore be suggested to be universally adaptable for not only hydrides but also other ionic compounds. The indicator is expected to be a key to find a relationship between material properties and crystal structures. Then, it could be a new guideline for designing hydrogen storage complex hydrides as well as a correlation between the electronegativity of metal cations and thermodynamic stability.

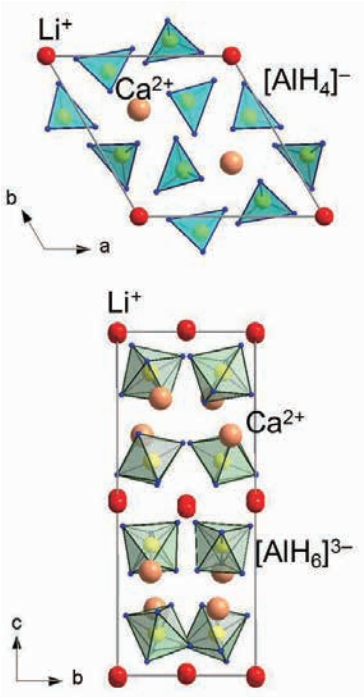

Fig. 2 Crystal structures of (top) $LiCa(AlH_4)_3$ and (bottom) $LiCaAlH_6$. In the crystal structure, Li, Ca and H atoms, $[AlH_4]^-$ and $[AlH_6]^{3-}$ are displayed as red, green, yellow and blue circles and cyan and green tetrahedra, respectively.

References

[1] S. Orimo, Y. Nakamori, J.R. Eliseo, A. Züttel and C.M. Jensen, Chem. Rev. 107, 4111 (2007).
[2] B. Bogdanović and M. Schwickardi, J. Alloys Compd. 253-254, 1, (1997).
[3] B.C. Hauback, Z. Kristallogr. 223, 636 (2008).
[4] Y. Nakamori, K. Miwa, A. Ninomiya, H.-W, Li, N. Ohoba, S. Towata, A. Züttel and S. Orimo, Phys. Rev. B 74, 045126 (2006).; K. Miwa, S. Takagi, M. Matsuo and S. Orimo, J. Phys. Chem. C 117, 8014 (2013).; S. Takagi, T.D. Humphries, K. Miwa and S. Orimo, Appl. Phys. Lett. 104, 203901 (2014).
[5] K. Tomiyasu, S. Sato and S. Orimo, Chem. Commun. 51, 8691 (2015).
[6] S. Takagi, Y. Iijima, T. Sato, H. Saitoh, K. Ikeda, T. Otomo, K. Miwa, T. Ikeshoji, K. Aoki and S. Orimo, Angew. Chem. Int. Ed. 54, 5650 (2015).
[7] G. Li, M. Matsuo, S. Deledda, B.C. Hauback and S. Orimo, Mater. Trans. 55, 1141 (2014).
[8] T. Sato, K. Tomiyasu, K. Ikeda, T. Otomo, M. Feygenson, J. Neuefeind, K. Yamada and S. Orimo, J. Alloys Compd. 584, 244 (2014).
[9] T. Sato, S. Takagi, M. Matsuo, K. Aoki, S. Deledda, B.C. Hauback and S. Orimo, Mater. Trans. 55, 1117 (2014).
[10] T. Sato, S. Takagi, S. Deledda, B.C. Hauback and S. Orimo, MH2014 Manchester, July 20–25, 2014.

Keywords: Crystallographic structure, Neutron diffraction, X-ray diffraction (XRD)
Shin-ichi Orimo (Hydrogen Functional Materials Division, Institute for Materials Research, Tohoku University)
E-mail: orimo@imr.tohoku.ac.jp
http://www.hydrogen.imr.tohoku.ac.jp/en/index.html

Fermi surface instabilities and superconductivity in uranium compounds

Superconductivity is one of the most interesting topics in the strongly correlated electron systems. There are many uranium-based heavy fermion compounds which show exotic superconductivity with anomalous pairing. We present our recent results on uranium heavy fermion superconductors, focusing on the Fermi surface instabilities and Lifshitz transition

After the discovery of superconductivity on UBe_{13}, many interesting actinide superconductors have been reported, such as odd-parity superconductivity, coexistence with antiferromagnetism, "high-Tc" superconductivity, superconductivity with strong Pauli paramagnetic effect. In particular, ferromagnetic superconductivity attracts much interest, because the unconventional pairing with spin-triplet state should be realized.

URhGe is a ferromagnet with the Curie temperature T_{Curie}=9.5K. Superconductivity coexists with ferromagnetism below T_{sc}=0.25K[1]. When the field is applied along the hard-magnetization axis (b-axis), field-reentrant superconductivity is observed between 8 to 13T. The upper critical field of conventional superconductivity is in general determined by the Pauli limit and the orbital limit. The Pauli limit of URhGe is very small below 0.5T, thus the reentrant superconductivity observed at extremely high field is indeed unconventional, and is most likely due to the spin-triplet state with equal spin-paring which is free from the Pauli limit. In order to study the mechanism of reentrant superconductivity, we focus on the Fermi surfaces, which reveal the electronic state from the microscopic point of view. Figure 1 shows the field dependence of Hall resistivity and thermopower[2,3]. The abrupt change in Hall resistivity and thermopower signal at H_R indicates the reconstruction of Fermi surfaces in URhGe near the reentrant superconducting phase. Increasing the magnetic field further, we detected the quantum oscillations both in the thermopower and in the magnetoresistance, namely, Shubnikov-de Haas effect. The frequency, which is proportional to the cross-sectional area of Fermi surface, is field-dependent, indicating the Fermi surface instabilities near the reentrant superconductivity.

Another important aspect for the mechanism of reentrant superconductivity is the field-induced ferromagnetic fluctuation[4]. Figure 2 shows the field dependence of the spin-spin relaxation rate, $1/T_2$, which corresponds to the longitudinal spin fluctuation. The divergence of $1/T_2$ at H_R is a direct microscopic evidence for the development of spin fluctuation near the reentrant superconductivity.

In URhGe, both ferromagnetic fluctuations and Fermi surface instabilities are the key ingredients for reentrant superconductivity.

We also clarified the Fermi surface instabilities and Lifshitz transition at high fields in other heavy fermion superconductors[5,6,7]. In the ferromagnetic superconductor UCoGe, we observed successive anomalies at 4, 9, 16, 21T for the field along the easy-magnetization c-axis. At all anomalies, significant change of quantum oscillation frequencies and the effective masses was observed, revealing

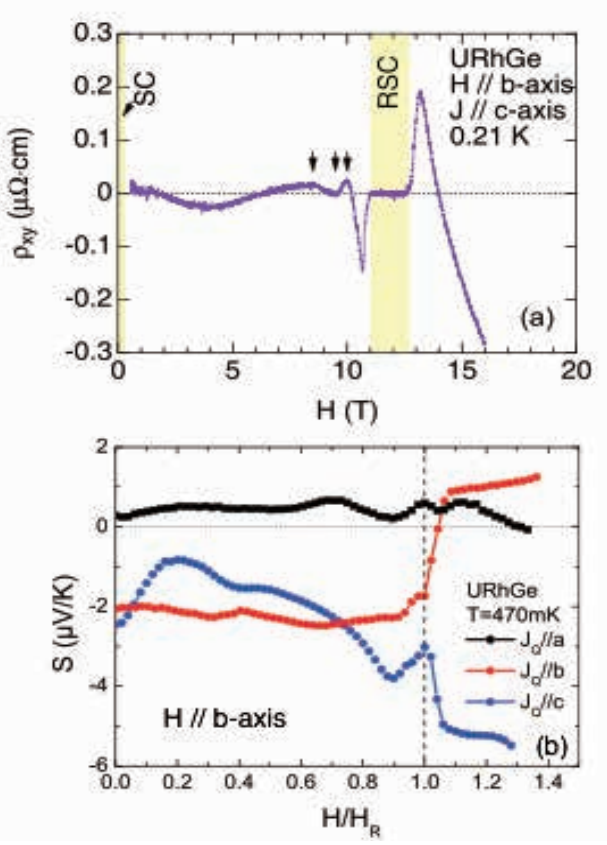

Fig. 1 Field dependence of Hall resistivity and thermopower for the field along b-axis in URhGe

the Fermi surface instabilities. This is consistent with the fact that UCoGe is a low carrier system with heavy quasi particles. In this case, the effective Zeeman energy is low, and the Fermi surfaces are easily changed by the magnetic field.
Uranium compounds have a large spin-orbit interaction and the dual nature of itinerant and localized 5f-electrons. Thus, small tuning parameters, such as magnetic field and pressure, can easily modify the ground state, and the novel quantum phase emerges.
This work was done in collaboration with A. Gourgout, G. Bastien, B. Wu, G. Knebel, A. Pourret, J. P. Brison, D. Braithwaite, J. P. Brison, J. Flouquet, I. Sheikin, Y. Tokunaga.

References

[1] D. Aoki, A. Gourgout, A. Pourret, G. Bastien, G. Knebel, J. Flouquet: C. R. Physique 15,(2014) 630.
[2] D. Aoki, G. Knebel, and J. Flouquet: J. Phys. Soc. Jpn. 83 (2014) 094719.
[3] A. Gourgout, A. Pourret, G. Knebel, D. Aoki, G. Seyfarth, and J. Flouquet: accepted for publication in Phys. Rev. Lett
[4] Y. Tokunaga, D. Aoki, H. Mayaffre, S. Kraemer, M.H. Julien, C. Berthier, M. Horvatic, H. Sakai, S. Kambe, and S. Araki: Phys. Rev. Lett. 114 (2015) 216401.
[5] G. W. Scheerer, W. Knafo, D. Aoki, M. Nardone, A. Zitouni, J. Beard, J. Billette, J. Barata, C. Jaudet, M. Suleiman, P. Frings, L. Drigo, A. Audouard, T. D. Matsuda, A. Pourret, G. Knebel, and J. Flouquet: Phys. Rev. B 89 (2014) 165107.
[6] A. Palacio Morales, A. Pourret, G. Knebel, G. Bastien, V. Taufour, D. Aoki, H. Yamagami, and J. Flouquet: Phys. Rev. B 93 (2016) 155120
[7] D. Aoki, G. Seyfarth, A. Pourret, A. Gourgout, A. McCollam,. J. A. N. Bruin, Y. Krupko, I. Sheikin: Phys. Rev. Lett. 116 (2016) 037202.

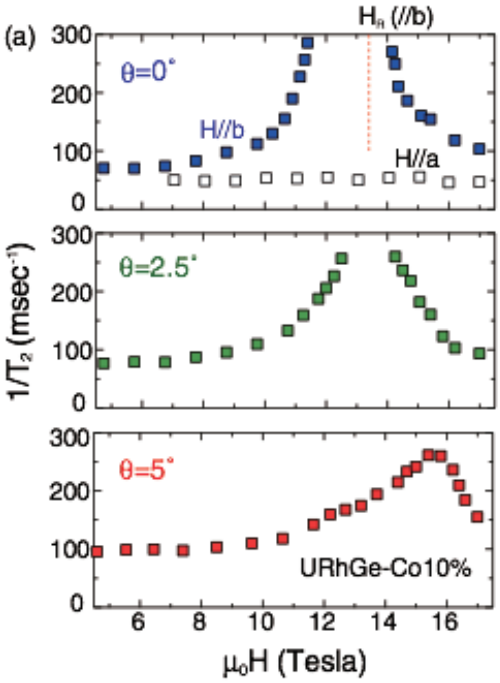

Fig. 2 Field dependence of spin-spin relaxation rate $1/T_2$ for H // b-axis in URhGe with 10% Co doping

Keywords: superconductivity, magnetism, actinide
Dai Aoki (Actinide Materials Science Division)
E-mail:aoki@imr.tohoku.ac.jp
http://actinide.imr.tohoku.ac.jp/

Developing a Terahertz-Frequency EPR Spectrometer

New type of THz-EPR spectrometer has been developed by combining a table top 30 T pulsed magnet and the single-shot detection-broadband THz radiation using spectral up-conversion technique. We have also investigated several new Ni and Co complexes by using the TESRA-IMR:ESR spectrometer installed at the Magnetism Division of IMR.

It has been recognized for a number of years that extending the frequency range of EPR spectrometers, that normally operate at microwave frequencies of 9.5 – 95 GHz, into the terahertz regime (1 THz = 1000 GHz) would have enormous benefits in terms of both spectral and temporal resolution. Recently, there has been a huge resurgence of interest in extending the frequency range of EPR spectroscopy, fuelled in-part by the advent of new terahertz radiation sources and detectors.

The aim of this proposal is to develop a compact laboratory-based EPR spectrometer that operates in the terahertz-frequency range and exploit its unique capabilities to probe next generation molecular magnetic materials. This will be achieved by combining an existing state-of-the-art laser-based terahertz time- domain spectrometer, developed by Dr Graham's group at the Photon Science Institute, with a portable high-field pulsed magnet developed by Prof Nojiri at the Institute of Materials Research.

Figure 1 (a) and (b) show the schematic view of the central part of the spectrometer and the photograph, respectively. The pulse magnet coil(not shown here) is set in the nitrogen bath with a vacuum-sealing pipe in the center. The THz- radiation goes through the central pipe. The sample is mounted on the sapphire cold finger pipe. The cold finger is attached to the He-gas flow type cryostat set side by side to the nitrogen bath. Temperature as low as several K is available with this setup. To adjust the shift of the sample by cooling, two cryostats are coupled by an adjustable bellow flange. Thanks to the short optical path, the adjustment can be done by a few supporting screws. The magnetic field up to 30 T is generated by the compact capacitor bank, which is developed and is assembled at IMR. The whole setup is easily mounted on the optical bench for its compactness. The capacitance, charging voltage and the storing energy of the bank are 8 mF, 2 kV and 16 kJ, respectively. The housing is 750X1100X1460 H and the weight is 350 kg. For the future upgrade, the voltage of the charger is set to 4 kV. The switching between the 2 kV and 4 kV modes can be made easily by the rearrangement of several solid busbars The extension of the capacitance can be made either by adding an extra capacitor box or by extending of the free-size Al-frame type housing.

(a)

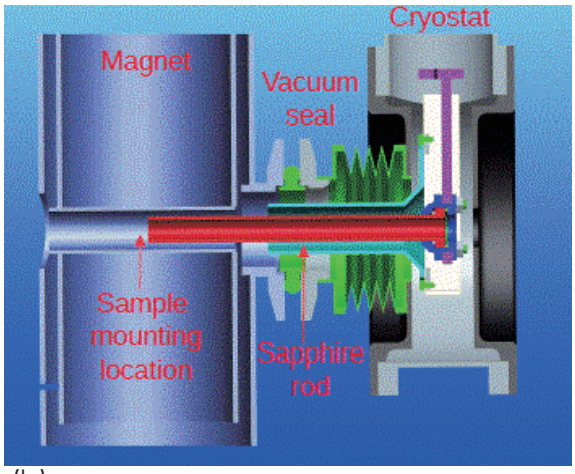

(b)

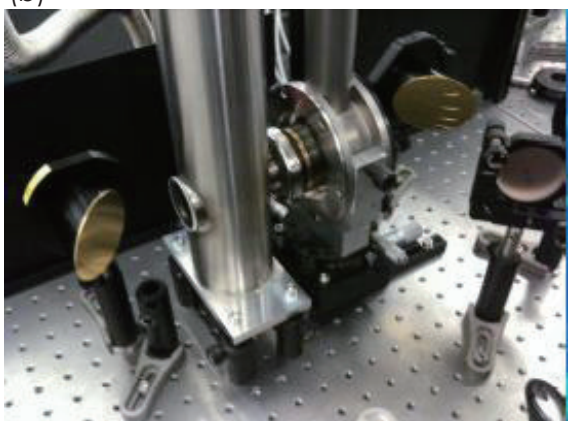

Fig.1(a) Schematic view of the nitrogen bath and the sample cryostat of the table top pulse magnet. Magnet coil is omitted.
Fig.1(b)Photo of the spectrometer setting on the optical bench.

The transmittance of the THz wave is measured between 0.1-3 THz. A sizable reduction of the transmission is found below 0.5 THz for the small opening angle of this system. A design to increase the angle to double that of the present system has been developed through the present collaboration and is now being commissioned. The key point of the upgrade is the use of a new nitrogen bath with the rectangular cross-section to minimize the optical path. It has the benefit to increase the nitrogen reservoir volume useful for longer operation time.

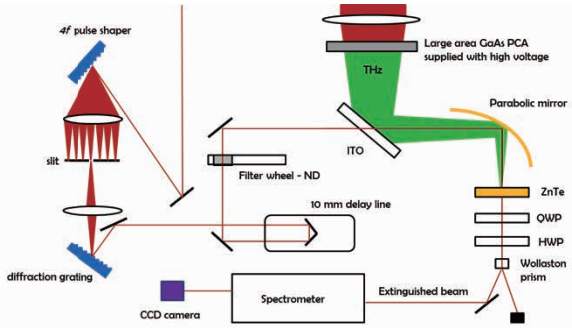

Fig. 2 Scheme of THz generation and detection.

(a)

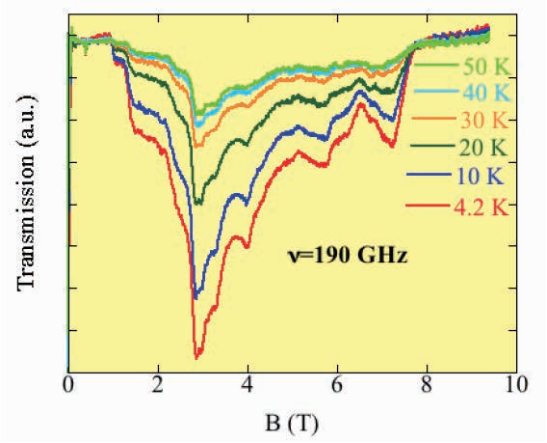

(b)

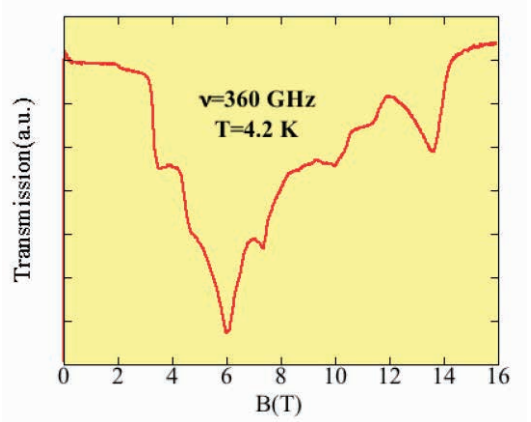

Fig. 3(a) Temperature dependence of EPR spectrum at 190 GHz measured by TESRA-IMR spectrometer. The broad multiple peaks are observed for the non- quenching orbital moment of Co ions.
Fig. 3(b) EPR spectrum at 360 GHz and at 4.2 K.

Figure 2 shows the schematic view of the single-shot broadband THz-generation scheme developed at Manchester University[1, 2]. The THz radiation spectrum can be measured as sidebands of the spectrum from a 100 fs amplifier with a central wavelength of 800 nm. A ZnTe crystal is used for up-conversion and the detection is made by using a single-grating spectrometer and CCD camera.

The THz spectrum has been obtained successfully by this scheme and the application for various materials is in progress.

We have also measured several Ni and Co based complexes at IMR. The purpose of this measurement is to compare the spectrum with THz-TDS and that of the conventional EPR.

Figure 3 (a) shows the temperature dependence of Co complex: $[Co_2(H_2O)(piv)_4(Hpiv)_2(3\text{-methylpyridine})_2]$ measured at 190 GHz. In the spectrum, seven strong peaks are found with nearly constant spacing. The center of the peak is located at 2.8 T which is related to g~4.5. The large g-value is typical for Co ions with non-quenched orbital moment.

The EPR spectrum at 360 GHz is shown in Fig. 3(b). The separation of peaks becomes much clear for the high resolution. Such improvement of the resolution indicates the advantage of THz EPR to the microwave EPR.

The temperature dependence of the spectrum is monotonic and the intensity decreases with increasing temperature. This behavior indicates that the observed EPR is the transition from the ground state and/or from the low energy excited states.

In summary, we have developed a broadband THz EPR spectrometer by using a single-shot THz detection scheme and a table-top pulsed magnetic field generator. For the complementary research, several magnetic complexes have been investigated with the THz monochromatic frequency EPR spectrometer.

References

[1] D. A. Walsh, D. M. Graham *et al.* Optics Express 22, p. 12028 (2014).
[2] D.M. Graham *et al.*, IEEE DOI:10.1109/IRMMW-THz.2014.6956078

Keywords: Electron spin resonance, High magnetic field, THz Spectroscopy
Darren M Graham(The Photon Science Institute, University of Manchester)
Hiroyuki Nojiri (Magnetism Division, IMR, Tohoku University)
E-mail: nojiri@imr.tohoku.ac.jp
http://www.hfpm.imr.tohoku.ac.jp

Activity Report

Workshops

FY 2014 Workshops

No.	Chairperson	Title of Workshop	Place	Date
14WS1	E. Saitoh	Spin Mechanics 2	IMR Lecture Hall	2014. 6.21-6.24
14WS2	H. Abe	2nd Asian Nuclear Fuel Conference (ANFC)	Sakura Hall, Tohoku University	2014. 9.18-9.19
14WS3	T. Goto	9th International Workshop on Biomaterials in Interface Science (Innovative Research for Biosis-Abiosis Intelligent Interface Summer Seminar 2014)	Zao, Miyagi	2014. 8.26-8.27
14WS4	T. Matsuoka	2nd Intensive Discussion on Crystal Growth of Nitride Semiconductors	IMRAM, Tohoku University	2014.10.30-10.31
14WS5	M. Fujita	Research Frontier of Transition-Metal Compounds Opened by Advanced Spectroscopies	IMR Lecture Hall	2014.9.30-10.2

ICC IMR International Workshop on Spin Mechanics 2

Spin mechanics is the science and engineering of the coupling of mechanics, i.e. the spatiotemporal behavior of the lattice degrees of freedom such as rotations and vibrations, with the spin degree of freedom in magnetic nanostructures. The 2nd International Workshop dedicated to this topic was held at the Institute for Materials Research of Tohoku University, 21–24 June 2014 under the auspices of the ICC-IMR and sponsored by the collaboration network "SpinNet" of the German DAAD and the "Reimei" program of the Japan Atomic Energy Agency, and others.

Fig. 1: Conference picture in the yard of the Institute for Materials Research.

According to Noether's theorem, rotational symmetry implies conservation of angular momentum. In a condensed matter system, any variation of the magnetization and therefore the intrinsic (spin) angular momentum of the many-body electron wave function in time and space is accompanied by a torque on the embedding lattice. This coupling between spin and lattice is the subject of the field of Spin Mechanics.

The ICC-IMR workshop on Spin Mechanics covered all aspects associated with this principle. Relevant topics include acoustically induced spin pumping, mechanical control of magnetic anisotropy, Einstein, de Haas, and Sagnac effects in nanostructures, and spin currents generated by rotation. Spin mechanics found applications in mechanical spin detection such as magnetic resonance force microscopy (MRFM). Spin-flip dissipation-induced mechanical torques have been predicted and measured. The magnon-phonon interaction is intimately related with the spin Seebeck effect. Ultrasound and surface acoustic wave-induced magnetization dynamics, spin-torque induced mechanical motion, nanoscale pumps and motors, magnetic resonance force microscopy, magnetically actuated NEMS, spin-induced fluid dynamics, spin torque motors, and quantum effects such as magnetic tunneling and magnon Bose condensation; all received attention.

The workshop consisted of tutorials, invited talks, and poster sessions. For details of the program, and sponsors we refer to the website spinmechanics2.imr.tohoku.ac.jp. It attracted 126 registered participants, 45 of whom came from 13 overseas countries. Due to the large interest of the community, the series of workshops that started in Tokai will be continued; Spin Mechanics 3 to be organized by the Technical University Munich in June 2015 (chaired by Dr. Sebastian Gönnenwein).

We thank all members of the organizing and local committees for their great dedication as well as all conference participants for their contributions and hope that the workshop will stimulate new exciting research and international collaborations.

Fig. 2: Spin Mechanics 2 logo.

Keywords: spintronics, mechanical properties, magnetic properties
Eiji Saitoh (IMR Tohoku University)
E-mail: eizi@imr.tohoku.ac.jp
http://www.imr.tohoku.ac.jp/ index.html

2nd Asian Nuclear Fuel Conference (ANFC)

The Asian Nuclear Fuel Conference (ANFC) is the tri-annual international meeting, which provides an international and academic forum for fundamental aspects of nuclear fuels, with collaborations among atomic energy societies of Japan, Korea and China. It successfully proceeded 18-19 September 2014 at Tohoku University. A total number of presented papers was 83. 100 people from 12 countries participated to this conference. ICC-IMR supported a portion of the financial support for the guest speakers from oversea countries to this conference.

Nuclear fuels such as cladding materials (Zr-base alloys) and inert fuel pellets (UO_2) are the key materials for nuclear reactors, and therefore mostly severe requirements are applied for safe operations. The Fukushima Dai-ichi nuclear accidents raised new fields of research and development in nuclear technology. For fuels, the investigations on reactor accidents are requested such as interactions between Zr and high temperature steam, mechanism of fuel melting process, and so on. Not only the investigations on accidents themselves, but also development of materials is requested as well as the plant designs both of which ensure higher safe performance. Especially for fuels scientifically reasonable and logical descriptions (mechanisms) are necessary.

Asian Nuclear Fuel Conference (ANFC) provides an international and academic forum for fundamental researches on all aspects of nuclear fuels. Following the successful 1st ANFC meeting 2012 in Osaka organized by Fuel Division of Atomic Energy Society of Japan (AESJ), 2nd ANFC meeting was held on 18 - 19 September 2014, Sendai, Japan. This meeting focused on establishing Asian communities in academic area, especially interaction among young researchers of universities and research institutions. Not only the fundamental researchers, but utilities and authorities shared the knowledge.

Total number of attendees were 100, including 28 students, from Japan (64), Korea (18), China (4), US (4), Taiwan (2), France (2), Germany (1), Switzerland (1), Russia (1), Sweden (1), Norway (1) and India (1). 30 Oral presentations, including 9 invited lectures, covered the following topics; Nuclear reactor accident analysis, Materials science and engineering in nuclear fuels and cladding in light-water reactors, fast breeder reactors and innovative reactors, as well as Spent fuel management and related chemistry. 41 poster presentations covered the above topics and others like severe accident code development. Student and young researchers' session was also held during the conference to develop new relationships in the community.

Through the above activities, the 2nd ANFC was successful to demonstrate the advanced activities in these fields. Development of advanced materials for anti-accident technology, atomic-level analysis by state-of-the-art microscopic technique and mechanical property measurement, advanced reprocessing technology and others were introduced and discussed thoroughly especially for the applications to Fukushima and accident-less reactor design.

The selected papers will be published in 2015 October issue of Journal of Nuclear Science and Technology [1].

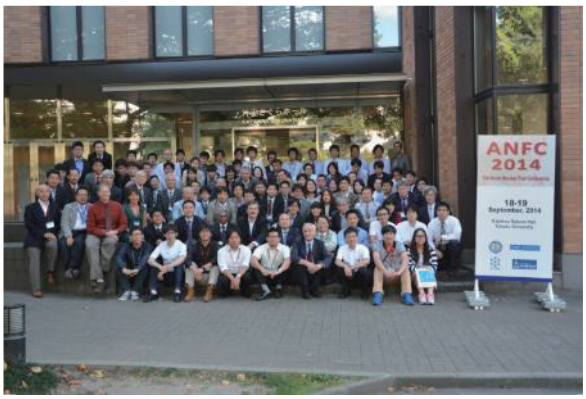

Fig.1 Conference photo

References

[1] Special issue of 2nd ANFC, J. Nucl. Sci. Tech. (2105) to be published.

Keywords: nuclear materials
Full Name: Hiroaki ABE (Nuclear Materials Engineering Division)
E-mail: abe.hiroaki@imr.tohoku.ac.jp
http://res.tagen.tohoku.ac.jp/~anfc2014/

9th International Workshop on Biomaterials in Biosis-Abiosis Intelligent Interface Science

- Innovative Research for Biosis-Abiosis Intelligent Interface Summer Seminar 2014 -

Development of Intelligent interface between human constituents and biomaterials is of importance because of strong demands for replacing various parts in human-body with artificial products. The experts, researchers and students from various fields related to biomaterials gathered at the 9th International Workshop on Biomaterials in Biosis-Abiosis Intelligent Interface Science 2014 on Aug. 26–27th at Sendai, Japan. The keynote lectures by three distinguished professors, invited lectures by three experts from abroad and 30 papers provided valuable opportunity for cross-over discussion, interdisciplinary idea sharing and new collaboration to develop and establish the intelligent interface science on biomaterials.

Interdisciplinary and international activities are necessary to develop the biomaterials, such as artificial bone and tooth, because the biomaterials should meet the various demands to control biofunctionalities and mechanical properties in a wide range from nano- to micro-scale, as well as compatibility with human body. Three Institute in Tohoku University, namely Institute for Materials Research (IMR), Graduate School of Dentistry and Graduate School of Biomedical Engineering, have been collaborating and involved the 5-year project on Biomaterials in Biosis-Abiosis Intelligent Interface Science. As the series of international forums in the frame this project, the 9th International Workshop on Biomaterials in Biosis-Abiosis Intelligent Interface Science 2014 in conjunction with Innovative Research for Biosis-Abiosis Intelligent Interface Summer Seminar 2014 was held on Aug. 26th–27th, 2014, at Miyagi Zao, Sendai.

The 2-days technical program in this workshop included 30 papers in which 3 keynote lectures and 3 invited lectures were given by distinguished professors and experts on biomaterials from Korea, China and Japan. About 70 participants of professors, researchers and students attended in the workshop.

Prof. Kiyoshi Koyano (Kyushu Univ.) provided a keynote lecture on establishment and maintenance of oral tissue-dental implant interface. The keynote lecture by Prof. Mitsugu Todo (Kyushu Univ.) was on osteochondral tissue engineering by hybridization of biocomposites and mesenchymal stem cells. Prof. Takao Hanawa (Tokyo Medical and Dental Univ.) gave a keynote lecture on Creation of biosis-abiosis intelligent interface. The state-of-the-art research was provided as invited lectures by three experts from abroad. The biological function and mechanisms of the protein Cpne7 was presented by Prof. Joo-Cheol Park (Seoul National Univ., Korea). Prof. Xing-quan Jiang (Shanghai Jiao Tong Univ., China) gave an invited lecture entitled "Application of structure and chemical cues in biomaterials design to regulate stem cells differentiation". Dr. Youngjin Cho (Korea Institute of Science and Technology, Korea) provided updated research on the next generation nano-bio fusion materials and interfaces. In addition to the lectures, the progress and present state of the collaborating 5-year project were introduced. Furthermore, presentations by speakers with various academic backgrouds provided valuable opportunity for sharing updated and interdisciplinary viewpoints and ideas to the all participants. The collaborative discussion had great contributions to the development on the intelligent interface science on biomaterials.

Fig. 1 Group photo and one shot in an invited lecture.

Keywords: biomedical, ceramic, metal
Takashi GOTO (Multi-Functional Materials Science)
E-mail: goto@imr.tohoku.ac.jp
http://interface2014.imr.tohoku.ac.jp/

2nd Intensive Discussions on Growth of Nitride Semiconductors

The international workshop "2nd Intensive Discussion on Growth of Nitride Semiconductors" was held at Sakura Hall, Katahira campus in Tohoku University on October 29-31. About 70 specialists in the field of nitride semiconductors participated in the workshop including foreign researchers. By using the method of the reverse engineering, researchers in both fields of devices and crystal growth presented each current status, and discussed on technical issues each other.

The international workshop "2nd Intensive Discussion on Growth of Nitride Semiconductors (IDGN-2)" was held on October 29-31 just after blue LEDs consisted of nitride semiconductors was awarded as "the 2014 Nobel Prize in Physics". The nitride semiconductors have been strongly expected to be applied for not only optical devices, but also electronic devices from the physical properties superior to conventional semiconductors such as Si and GaAs [1], because of energy saving and generation for realizing the sustainable society. In this meaning, this workshop aimed to clarify the requests from high-efficient optical devices including white LEDs, and electronic devices such as high-power, high-breakdown voltage, and high frequency transistors to crystal growers, from the viewpoint of the reverse engineering. This is the main concept and the feature of this workshop. The workshop also had an important aspect; i.e., the growers of bulk GaN and epitaxial films presented up-to-date technologies to device fabricators. We believed that mutual communication between crystal growers and device fabricators could bring a new era beyond the current technical limitation.

The previous workshop (IDGN-1) held in 2012 provided us the opportunity to share the most recent achievements and to discuss the technical issues on crystal growth and device applications of nitrides. In the present workshop, we newly arranged technical sessions to cover electronic devices, optical devices and their related crystal growth techniques. The selected speakers are invited as a worldwide specialist in each topic.

We had seven sessions on high power and high breakdown voltage transistors, high frequency transistors, epitaxial growth and process technology for transistors, optical devices, epitaxial growth for optical devices, and crystal growth. Domestic and foreign key-persons presented their new results and future perspectives. Discussion made the time pass quickly.

In this workshop, we intended to have "Intensive discussion", therefore, the number of participants were limited to 70 people.

The workshop chairs found a great deal of satisfaction in all the topics, and would like to say thank all the panelists and participants who boosted the fruitful discussions.

This workshop was supported by IMR and IMRAM.

References

[1] Selected Topics in Applied Physics "Progress of Nitride Semiconductors and their Future Prospects", ed. T. Matsuoka et al., Jpn. J. Appl. Phys., vol. 53, No. 10, Oct. 2014.

Fig. 1 Participants near the venue in Katahira campus

Keywords: nitride, crystal growth, epitaxy
Takashi Matsuoka (Physics of Electronic Material, IMR)
E-mail: matsuoka@imr.tohoku.ac.jp
http://www.matsuoka-lab.imr.tohoku.ac.jp/

Research frontier of transition-metal compounds opened by advanced spectroscopies

Novel science brought through new materials and the spectroscopic measurements were discussed in this workshop. The state-of-the-arc techniques such as he time-resolved spectroscopy, which potentially uncovers the magnetization dynamics of domain wall and Skyrmions, were reported. The complementally use of quantum beams at large facilities for the newly discovered materials was also discussed.

In transition-metal compounds, various novel quantum phenomena emerge from the interplay of charge, spin, and orbital degrees of freedom with lattice vibration. Behind the phenomena, there are novel electronic states controlled by multi-scale dynamics over energy and space. It is, therefore, important to understand their electronic states by spectroscopic tools scanning a wide range of energy as well as real and momentum spaces. To discuss a future direction and make a progress in the research field of transition metal compounds, we held an international workshop "Research frontier of transition-metal compounds opened by advanced spectroscopies" on Sep. 30rd-Nov. 2nd, 2014 at Institute for Materials Research, Tohoku Univ.

We selected following topics as the main target.

1: Skyrmion and magnetic domain wall,
2: Strong spin-orbit coupled systems, e.g., Iridates, magnetostriction and negative thermal expansion,
3: High-Tc superconductivity in cuprate oxides and related phenomena,
4: Superconductivity in Fe-based compound and the mechanism.

The advanced spectroscopic technique also discussed. In particular, we focus on time-resolved spectroscopy, which is being advanced very quickly in the world followed by the development of femtosecond laser and free electron laser.

This workshop provided a unique opportunity to discuss a different type of spectroscopy measurements and exchange the ideas on recent and long-standing researches. More than 100 people, including a lot of students and young researchers, took part in the workshop, and the workshop received a favorable impression. We would like to thank all participants and the support from ICC-IMR for the successful workshop.

Fig. 1 A group photo of workshop. More than 100 researchers including many young scientists participated in the workshop.

Keywords: high-tc iron-based pnictide superconductivity, electronic material, neutron scattering
Masaki Fujita (Material Processing and Characterization Division)
E-mail: fujita@imr.tohoku.ac.jp
http://www.qblab.imr.ac.jp/ index.html

Activity Report

KINKEN WAKATE

FY 2014 KINKEN WAKATE

No.	Chairperson	Title of Workshop	Place	Date
14Wakate	M. Fujita	11th Materials Science School for Young Scientists (KINKEN-WAKATE 2014),	IMR Lecture Hall	2014.9.29

Kinken Wakate: "11th Materials Science School for Young Scientists Fundamentals and Modern Aspects of Superconductivity"

Kinken Wakate was held on 29th September 2014 at Institute for Materials Research. This year four professors provided lectures on superconductivity from both of theoretical and experimental points of view. In short talk session, several participants gave presentation on their projects and enjoyed fruitful discussion with senior professors.

Superconductivity is one of most fascinating topics in condensed matter physics. Huge amount of researches on the superconductivity have been accumulated since the discovery in Mercury about a hundred years ago. The KINKEN WAKATE school was organized to give young students and scientists a great opportunity to learn fundamentals and modern aspects of superconductivity. Four world-famous professors were invited and gave lectures on superconductivity. Over 40 students and scientists participated the school and learned wide variety of topics in superconductivity.

The lecture started from Prof. Shin-ichi Uchida's lecture "Road to Higher Tc" and he explained key parameters for the high-Tc superconductivity in copper oxides and iron compounds. Prof. Martin Greven gave a lecture "Neutron Scattering Studies and the Phase Diagram of the Cuprate High-Temperature Superconductors" and reviewed the rich phase diagram of cuprate high-Tc superconductors obtained mainly from neutron scattering technique. Prof. Yasutomo. J. Uemura gave the lecture "Muon Spin Relaxation Studies of Unconventional Superconductors" and discussed the paring mechanism of various unconventional superconductors from view of superconducting symmetry. Finally, Prof. Oleg P. Sushkov gave the lecture "Magnon Mediated Superconducting Pairing in a Very Lightly Doped Two Dimensional Mott Insulator" and talked theoretical description of pairing mechanisms in strongly-correlated electron systems. Throughout the lecture questions and answers were exchanged actively. In short talk session, several participants gave a contributed presentation on their research. Senior scientists kindly made constructive suggestions and comments on their talks. They enjoyed the fruitful discussion overrunning the scheduled time. The school was concluded in great success.

Fig. 1 A scene of the lecture.

Fig. 2 Group photo.

Keywords: Superconducting
Masaki Fujita (Metal Physics with Quantum Beam Spectroscopy)
E-mail: fujita@imr.tohoku.ac.jp
http://qblab.imr.tohoku.ac.jp

Activity Report

Short-term Visiting Researchers

FY 2014 Short-term Visiting Researchers

Application No.	Name	Host	Proposed Research	Title	Affiliation	Term
14SV1	Atsufumi Hirohata	K. Takanashi	Experimental Demonstration of a Persistent Current	Reader	University of York, UK	2014. 9.28-10.9
14SV2	Albrecht Jander	K. Takanashi	Study of Magnetostriction in FePtPd Alloys	Assoc. Professor	Oregon State University, USA	2014.6.17-7.25
14SV3	Syamak Hossein Nedjad	T. Furuhara	Recrystallization Behavior and Grain Refinement Efficiency of Deformed Acicular Frrite and Lath Martensite Structures of C-Mn Steel	Assoc. Professor	Sahand University of Technology, Iran	2014.11.9-11.30
14SV4	Andrey Medvedev	A. Yoshikawa	Research about Piezoelectric Crystals and Development of Novel Piezoelectric Devices	Technical Director	JSC Fomos Materials, Russia	2014.9.26-10.29
14SV5	Dorthe Bomholdt Ravnsbaek	S. Orimo	Development of New Complex Hydrides with Sodium Fast-Ionic Conductivity	Assistant Professor	University of Southern Denmark, Denmark	2015.1.9-1.18
14SV6	Takuya Yamamoto	K. Nagai	Dose Rate Effects on Microstructure and Hardening in Ion and Test Reactor Irradiated RPV Steels	Professional Research Engineer	University of California Santa Barbara, USA	2014.12.5-12.22
14SV7	Vladimir Kochurikhin	A. Yoshikawa	Novel Material Concepts for Rare Earth-Free Scintillators and Phosphors	Head of Research Laboratory	General Physics Institute, Russia	Dr.Vladimir Kochurikhin 2014.11.28-12.14 2015.2.7-2.20 Prof. Georges Boulon 2015.2.8-2.17
14SV8	Michael Zhitomirsky	H. Nojiri	Theory of Low-Dimensional Frustrated Magnets-Application to $MnWO_4$	Staff Scientist	Institute of Nanoscience and Cryogenics, C.E.A. Grenoble, France	2015.2.18-3.1

Experimental Observation of a persistent current

We intend to demonstrate an alternative method of generating a spin-polarized persistent current in a non-magnet by introducing a non-uniform magnetic field from an epitaxial FePt nanopillar with perpendicular magnetic anisotropy. Even though such a spin-polarized persistent current was proposed theoretically almost 20 years ago [1], there has been no experimental demonstration to date. This device is expected to open up new research horizons as a spin source for quantum computation.

The quantum phases of charged particles in mesoscopic structures have been investigated intensively. Their interference and oscillatory behaviors were induced by application of an external field [2]. Electrons traveling along semiconductor or normal metal rings threaded by a magnetic flux acquire a quantum dynamical phase that produces interference phenomena such as the Aharonov-Bohm (AB) and Altshuler-Aronov-Spivak (AAS) effects. In addition, when the spin of the electron rotates during its orbital motion along the ring-shaped path, the electron acquires an additional phase element known as the geometrical or Berry phase.

A new nanofabrication method has been developed to produce a quantum device on a MgO(001) substrate consisting of a non-magnetic nanoring (inner diameter: 200, 260, 300 and 350 nm in design) with an FePt nanopillar (diameter: 120, 180, 220 and 270 nm in design) inside by a combination of electron-beam lithography and Ar-ion milling. The nanoring is 150 nm wide and contains a 20-nm-thick Ag or Cu layer without any Cr adhesion layers onto the MgO substrate by an improved deposition technique. This allows us to avoid any spin-polarized electron flow in the Cr layer.

As shown in Fig. 1, the center nanopillar is designed to provide a nonuniform magnetic field in the nanoring in its remanent state after perpendicular saturation. Such a nonuniform field is theoretically expected to induce a persistent spin current in the nanoring [1]. Four contacts were fabricated near the nanoring for measurement of the induced current. In our improved design, with and without 10 nm off-set was introduced for the nanopillar to control the nonuniformity of the fields.

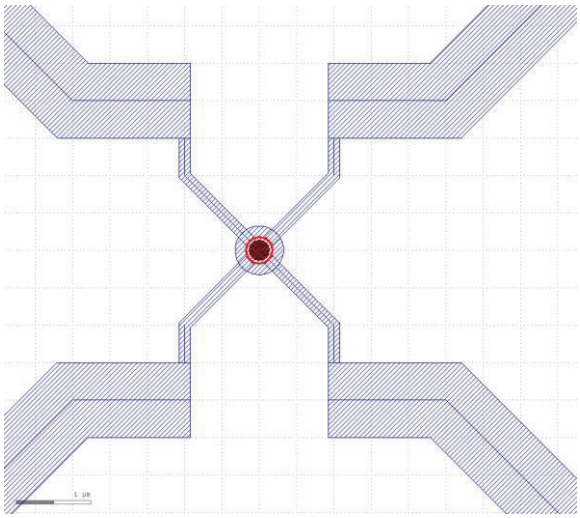

Fig. 1 Design of the quantum device fabricated in this project. The red dot represents the FePt nanopillar and the purple ring and wires represent the Ag and Cu nanowires.

In summary, we have successfully designed a new quantum device consisting of a ferromagnetic FePt nanopillar enclosed by a nonmagnetic nanoring. We have been measuring these devices using a dilution refrigerator at Osaka University.

References

[1] D. Loss and P.M. Goldbart, *Phys. Rev. B* **45**, 13544 (1992).
[2] Y. Imry, *Introduction to Mesoscopic Physics* (Oxford Univ. Press, Oxford, 1997).

Keywords: spin current,magnetoresistance (transport), nanostructure
Full Name (Division Name or Affiliation)
E-mail: atsufumi.hirohata@york.ac.uk
http://www-users.york.ac.uk/~ah566/

Study of Magnetostriction in FePtPd

This work studied magnetostriction in $L1_0$ ordered $Fe_{50}Pt_{(50-x)}Pd_x$ alloy thin films with varying Pd content. The measurements of the sputter-deposited films, performed using the cantilever bending technique, indicate that the magnetostriction is dependent on the film composition and a maximum magnetostriction of 28 ppm is found in the $Fe_{50}Pt_7Pd_{43}$ film. These results suggest the possibility of tailoring magnetostriction via film composition for energy assisted data storage and synthetic multiferroic random access memory applications.

FePtPd alloy films, with strong perpendicular magnetic anisotropy, are leading candidates for recording media in next-generation hard disk drives and solid state multiferroic random access memory technologies. The magnetostrictive properties of such materials are of importance, as strain can be used to manipulate their magnetic anisotropy and therefore their magnetic switching characteristics.

The 100 nm thick $Fe_{50}Pt_{(50-x)}Pd_x$ films were deposited on 0.5 mm thick single crystal MgO (100) substrates. The films were prepared by co-sputtering from three independent targets. The sputtering power to the Pd and Pt targets was adjusted to obtain films with different compositions. $L1_0$ ordering was confirmed by X-ray diffraction measurements.

The in-plane and out-of-plane hysteresis loops of the samples were measured by SQUID magnetometry. These confirmed the desired strong perpendicular magnetic anisotropy.

The magnetostriction of the samples was determined using the cantilever bending method illustrated in Fig. 1. The FePtPd film is on the bottom of the cantilevered MgO substrate. To measure the magnetostriction

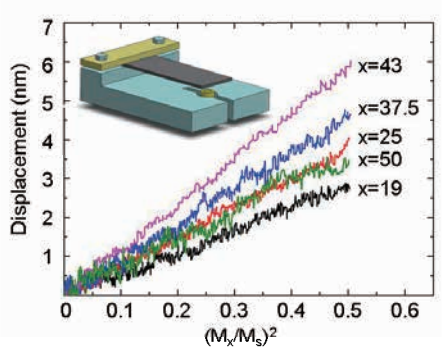

Fig. 1 Illustration of the cantilever bending method for magnetostriction measurement and resulting cantilever displacements plotted as a function of the magnetization for samples of different Pd content, x.

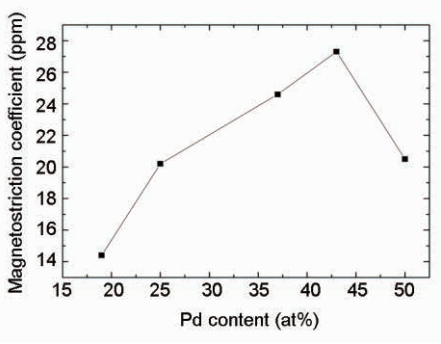

Fig. 2 Magnetostriction coefficient as a function of Pd content for $Fe_{50}Pt_{(50-x)}Pd_x$ thin films.

in the film, an in-plane magnetic field varying from 0 T to 5 T is applied along the cantilever. The dimensional change induced in the film through its magnetostrictive effect results in the deflection of the free end of the cantilever. This displacement is measured by a capacitive displacement sensor and plotted as a function of the magnetization, for films of various compositions in Fig. 1.

Using elastic theory and material properties of the cantilever and film, the magnetostriction coefficient of the films were derived from the displacement data. The magnetostriction coefficients for the FePtPd films are plotted in Fig. 2 with respect to the Pd content of the alloy.

These results have been presented at the 2015 IEEE International Conference on Magnetism and an associated manuscript is currently under review for the IEEE Transactions on Magnetics [1].

References

[1] W. Li, W. Zhou, P. Lenox, T. Seki, K. Takanashi, A. Jander, and P. Dhagat, "Magnetostriction Measurements of L10 $Fe_{50}Pt_{(50-x)}Pd_x$ Thin Films", presented at the IEEE International Magnetics Conference, Beijing, China, May 2015; To be published in IEEE Transactions on Magnetics.

Keywords: $L1_0$ FePt, magnetic properties, mechanical properties
Albrecht Jander (Oregon State University)
E-mail: jander@eecs.oregonstate.edu
http://oregonstate.edu/engr/magnetics/

Behavior and Grain Refinement Efficiency of Deformed Acicular Ferrite and Lath Martensite Structures of C-Mn Steel

Subcritical recrystallization microstructure of partially homogenized and isothermally transformed Fe-2.5Mn-0.18C-0.03Ti (mass%) steel was studied by means of electron probe microanalysis (EPMA), optical microscopy and electron back scattered diffraction (EBSD). Isothermal transformation of austenite at 823 K for 1.8 ks produced Widmansttaten microstructure which turns to a duplex ferrite-austenite microstructure after cold rolling and recrystallization at 923 K for 3.6 ks.

Grain refinement efficacy of cold rolled and recrystallized low carbon steels is substantially enhanced by preliminary phase transformations [1]. For example, it has been shown that cold rolling and annealing of lath martensite gives rise to effective grain refinement [2]. Hossein Nedjad et al. [4] studied the grain refinement and tensile properties improvement of cold rolled and annealed acicular microstructures of Fe-C-Mn steels. A duplex microstructure consisting of Widmansttaten ferrite laths and martensite, obtained by isothermal transformation of austenite in a partially homogenized Fe-2.47Mn-0.18C-0.03Ti (mass%) steel, showed remarkable grain refinement and tensile properties improvement. Fig. 1 shows optical micrograph of the as-transformed microstructure. Supplementary optical microscopy, electron back scattered diffraction (EBSD) and electron probe microanalysis (EPMA) were used presently for better understanding of the as-transformed and recrystallized microstructures.

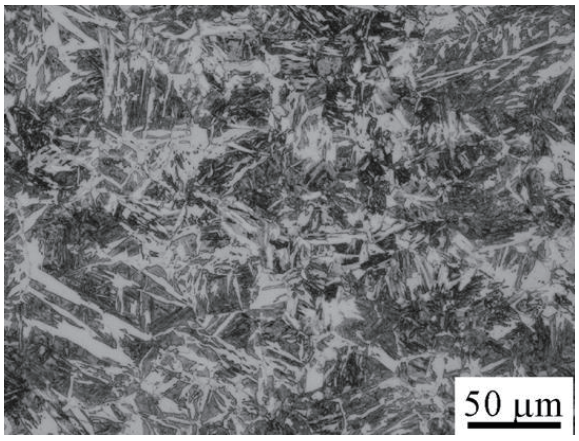

Fig. 1 Optical micrograph showing microstructure isothermally transformed for 1.8 ks at 823 K.

EPMA indicated heterogeneities in Mn distribution resulted from incomplete homogenization treatment. EBSD identified Kurdjamov-Sachs orientation relationship between ferrite laths and parent austenite phase.

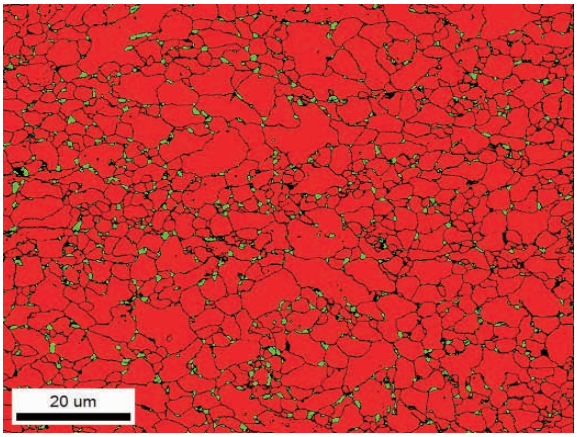

Fig. 2 EBSD phase mapping of austenite particles (green-coloured phase) and new ferrite grains (red-coloured matrix phase) in a specimen annealed for 3.6 ks at 923 K after cold rolling.

Discontinuous nucleation of occasional new ferrite grains and retention of fine austenite particles were found in a specimen annealed for 3.6 ks at 873 K after cold rolling. After annealing for 3.6 ks at 923 K, recrystallization takes place completely. Fig.2 shows an EBSD phase mapping of austenite particles (green-coloured phase) and new ferrite grains (red-coloured matrix phase) of the latter. Calculation of phase diagrams indicated that solute-enriched zones resulted from incomplete homogenization in association with solute partitioning during isothermal transformation possibly encounter subcritical annealing regime which leads to austenite reversion during annealing. The results adopt recrystallization behavior under practical conditions of incomplete homogenization in industrial rolling mills.

References

[1] N. Tsuji and T. Maki, Scripta Mater. 60, 1044-1049 (2009).
[2] R. Ueji, N. Tsuji, Y. Minamino and Y. Koizumi, Acta Mater. 50, 4177-4189 (2002).
[3] S. Hossein Nedjad, Y. Zahedi Moghaddam, A. Mamdouh Vazirabadi, H. Shirazi and M. Nili Ahmadabadi, Mater. Sci. Eng. A 528, 1521-1526 (2011).

Keywords: steel, grain size, electron microscopy
Syamak Hossein Nedjad (Materials Engineering, Sahand University of Technology, Iran)
E-mail: hossein@sut.ac.ir
http://mae.sut.ac.ir/showcvdetail.aspx?id=9

Application of $Ca_3TaGa_3Si_2O_{14}$ single crystal in New Types of Modern Piezoelectric Devices

Piezoelectric filter based on $Ca_3TaGa_3Si_2O_{14}$ single crystals operating in a thickness shear mode was manufactured. The filter based on the crystal elements with angle cut 21°20' has frequency deviation less than 120 ppm in the operating temperature range from −40 up to 80°C.

Recently, new piezoelectric crystals that also operate at high temperatures have been introduced in wide bandwidth acoustic wave filters, frequency control, and high-temperature sensor applications. The study, production, and application of langasite family crystals have been rapidly developing in recent years. This crystal group is isostructural to $Ca_3Ga_2GeO_{14}$ and currently it includes around 100 compounds. One of the langasite family crystals is calcium tantalum gallium silicate ($Ca_3TaGa_3Si_2O_{14}$, CTGS).

CTGS single crystal belongs to the trigonal system (space group P321, point group 32) and shows peculiar properties such as low dependence of dielectric and electromechanical properties from temperature. Also, its large magnitude of piezoelectric modulus d_{14} = 13.25 pC/N allows to obtain high values of the coupling factor for different types of motion.

Fig.1 shows the variations of the coupling factor as functions of the rotation angle Ψ around X-axis for different kinds of vibration mode. The maximum value of the coupling factor k12 for extensional mode is close to 24.8% observed for the angle Ψ= - 37°. For rotated X-cut operating in a face shear mode the largest coupling factor k14 equals 23.96%.

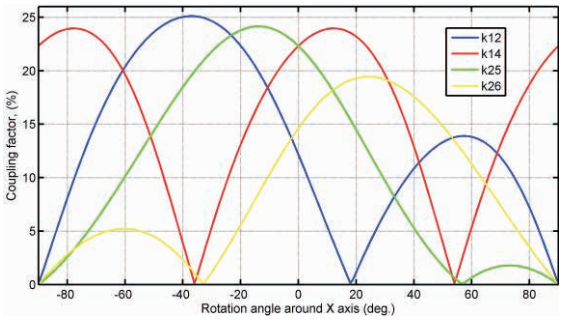

Fig. 1 Coupling factors as functions of rotation angle Ψ

As was shown in [1], [2] and observed from Fig.1 the coupling factor k26 of thickness shear mode for temperature compensated cut YXl/21°20´ is close to 19%.

Using this cut a piezoelectric filter at nominal frequency 12 MHz with pass band width 75 kHz was manufactured. Fig.2 shows the typical attenuation characteristic of the filter. The deviation of cut-off frequencies was less than 1.5 kHz in the temperature range from −40 up to 80°C.

Fig. 2 Attenuation characteristic of CTGS filter

CTGS shows great potential and properties useful for resonators and filters based on temperature compensated cut at room temperature.

References

[1] F. Yu, S. Zhang, X. Zhao, D. Yuan, L. Qin, "Investigation of $Ca_3TaGa_3Si_2O_{14}$ piezoelectric crystals for high temperature sensor," J. Appl. Phys. 109, 114103, 2011.

[2] A. Medvedev, S. Sakharov, Investigation of the Electrode Coating Influence on the Frequency Temperature Characteristics of the Resonators Operating at the Rotated Y-Cut Ca3TaGa3Si2O14 Single Crystals, Joint UFFC, EFTF and PFM Symposium, 2013, p. 114-117

Keywords: crystal, piezoelectric, devices.
Full Name: Andrey Medvedev, OAO "Fomos Materials"
E-mail: medvedev@imr.tohoku.ac.jp
http://www.newpiezo.com

Development of new complex hydrides with sodium fast-ionic conductivity

Complex hydride $Na_2(BH_4)(NH_2)$ can be a potential candidate for solid electrolytes for next-generation sodium ion batteries due to the high sodium ionic conductivity and high electrochemical stability. In this study, we have experimentally investigated the effect of chloride substitution in $Na_2(BH_4)(NH_2)$ on the ionic conductivity.

We have reported that the complex hydride $Na_2(BH_4)(NH_2)$ consisting of Na^+, $[BH_4]^-$ and $[NH_2]^-$ exhibits sodium fast-ionic conductivity at room temperature because of the specific antiperovskite-type structure with vacancies in the Na^+ site [1]. We have also found that substitution of halide ions such as Cl^- for $[BH_4]^-$ and $[NH_2]^-$ is effective to enhance lithium ionic conductivities of Li-based complex hydrides in our previous studies [2]. In this study, we have experimentally investigated the effect of chloride substitution in $Na_2(BH_4)(NH_2)$ on the ionic conductivity.

$Na_2(BH_4)(NH_2)$ and NaCl were mechanically milled in the molar ratio of 9 : 1, followed by heat treatment at 180 °C under Ar. Figure 1 compares the powder X-ray diffraction profiles of $Na_2(BH_4)(NH_2)$ and $9Na_2(BH_4)(NH_2)$ + NaCl. The diffraction peaks of the antiperovskite-type structure shifted to higher angle clearly for $9Na_2(BH_4)(NH_2)$ + NaCl. The result suggests that although small amount of unknown phase was also included, the $[BH_4]^-$ complex anions were partially substituted by Cl^- in $9Na_2(BH_4)(NH_2)$ + NaCl, judging from the ionic radii of $[BH_4]^-$ (2.05 Å), $[NH_2]^-$ (1.68 Å) and Cl^- (1.68 Å).

The sodium ionic conductivity of $9Na_2(BH_4)(NH_2)$ + NaCl was measured by ac impedance method in the temperature range from 27 °C to 150 °C, as shown in Figure 2. The ionic conductivity of $Na_2(BH_4)(NH_2)$ was as high as 2×10^{-6} S/cm at 27 °C and it increased with increasing temperature. However, $9Na_2(BH_4)(NH_2)$ + NaCl showed one-tenth lower ionic conductivity than $Na_2(BH_4)(NH_2)$.

We have recently found out a strong correlation between reorientational motion of complex anions and mobility of cations in complex hydrides [3]. The smaller crystal lattice of $9Na_2(BH_4)(NH_2)$ + NaCl due to the partial substitution of Cl^- for $[BH_4]^-$ may make the reorientational motions of $[BH_4]^-$ and/or $[NH_2]^-$ slower, which could result in the lower ionic conductivity by heightening the Na^+ diffusional barrier. We will accomplish the higher ionic conductivity by substitution of larger halide ions such as I^- in the near future.

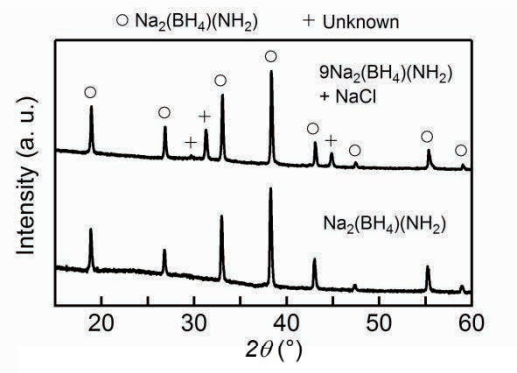

Fig. 1 X-ray diffraction profiles of $Na_2(BH_4)(NH_2)$ and $9Na_2(BH_4)(NH_2)$ + NaCl.

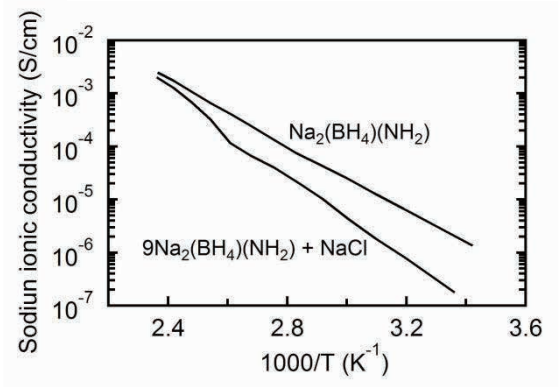

Fig. 2 Temperature dependences of ionic conductivities of $Na_2(BH_4)(NH_2)$ and $9Na_2(BH_4)(NH_2)$ + NaCl.

References

[1] M. Matsuo, S. Kuromoto, T. Sato, H. Oguchi, H. Maekawa, H. Takamura and S. Orimo, Appl. Phys. Lett. 100, 203904 (2012).

[2] M. Matsuo and S. Orimo, Adv. Energy Mater. 1, 161 (2011).

[3] T.J. Udovic, M. Matsuo, W.S. Tang, H. Wu, V. Stavila, A.V. Soloninin, R.V. Skoryunov, O.A. Babanova, A.V. Skripov, J.J. Rush, A. Unemoto, H. Takamura and S. Orimo, Adv. Mater. 26, 7622 (2014).

Keywords: ionic conductor, reactive ball milling

Dorthe Bomholdt Ravnsbaek (University of Southern Denmark)
Motoki Matsuo (Collaborative Research Center on Energy Materials / Hydrogen Functional Materials Division)
E-mail: mmatsuo@imr.tohoku.ac.jp
http://www.hydrogen.imr.tohoku.ac.jp/

Dose Rate Effects on Microstructure and Hardening in Ion and Test Reactor Irradiated Reactor Pressure Vessel (RPV) Steels

Formation of displacement cascade-induced defects, cascade fragments (CF), in RPV steels, which can be enhanced in accelerated irradiations at high dose rates, was examined using ion irradiation, nano-indentation and atom-probe tomography. Radiation enhanced precipitation of Cu-Ni-Mn-Si clusters is significantly delayed at the high dose rate of ≈ 10^5 dpa/s, while at the same time non-Cu dependent large hardening is observed, which can be accounted for by the formation and spatial saturation of CFs.

Irradiation embrittlement of RPV steels, typically characterized by brittle to ductile transition temperature shift (TTS), must be accurately predicted for safe reactor operation. The current TTS prediction model under-predicts many high neutron fluence (ϕt) data mostly obtained in test reactor irradiations. This is partially due to cascade fragments (CF) formed in aged displacement cascades, which anneal continuously during reactor operation, but build up at high flux (ϕ) in test reactors. The CFs also enhance point-defect recombination, that delays radiation enhanced precipitation hardening and embrittlement. The objective of the research is to understand and build mechanistic models of defect formation in RPV steels irradiated at very high dose rate – neutron flux (ϕ) range ϕ > 10^{13} n/cm^{2}s or corresponding dpa (displacement per atom) rate greater than ≈ 10^{-8} dpa/s.

RPV model steels with systematically varied Cu and Ni contents were irradiated by Fe^{2+} ions with 2.8MeV energy at 290°C to 0.005 to 0.2 dpa at a dose rate of ≈ 10^{-5} dpa/s as a nominal value defined at the depth of 500 nm. Nano-hardness and atom-probe tomography measurements have been carried out for some of the steels.

Figure 1 shows atomprobe elemental maps of a 0.4%Cu-1.3%Ni-1.4%Mn steel irradiated to 0.2 dpa at two different dose rates: a) 10^{-5}; and b) $1.5x10^{-7}$ dpa/s. Cu rich solute cluster formation is significantly delayed at higher dose rate. Similar delay is also observed in other alloys. Figure 2 shows the volume fraction of precipitates formed in a 0.4%Cu-0.8N%Ni-1.4%Mn steel irradiated in reactors as well as by ions at various dose rates. Fastest precipitation trend is observed at 10^{-10}~10^{-9} dpa/s followed by 10^{-8}~10^{-7} dpa/s while significant delay is observed at the highest dose rate of ~10^{-5} dpa/s in ion irradiation. In spite of the delay in precipitation, significant hardening is observed, which for example reaches ΔH ≈ 300 MPa at 0.2 dpa in a 0%Cu steel. As illustrated in Figure 3, our growing database of ion irradiation hardening shows that 0, 0.1 and 0.2Cu steels show similar large hardening at low dose ion irradiation regardless the Cu content. It cannot be accounted for by precipitates or loops, but a CF hardening model including spatial saturation of the CFs at extremely high dose rates gives good representation of the trends. Residual hardening at higher dose is also consistent with precipitation hardening trend at lower dose rates when the recombination effects are taken into account.

Further study including positron annihilation with post irradiation annealing will be carried out when slow positron beam equipment in Oarai Center is recovered from the breakdown.

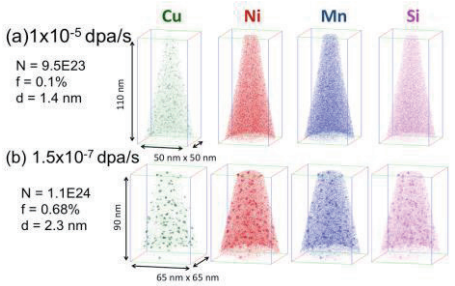

Figure 1 Atom probe elemental maps of 0.4Cu-1.3Ni-1.4Mn steel irradiated to 0.2 dpa at a) $1x10^{-5}$ dpa/s by Fe^{2+} ions and b) $1.5x10^{-7}$ dpa/s in BR2 test reactor, showing significant delay in cluster formation at higher dose rate.

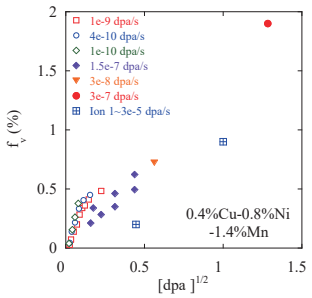

Figure 2 Volume fraction of Cu-Ni-Mn-Si precipitate in 0.4% Cu-0.8% Ni-1.4%Mn steel formed by radiation enhanced diffusion at various dose rates.

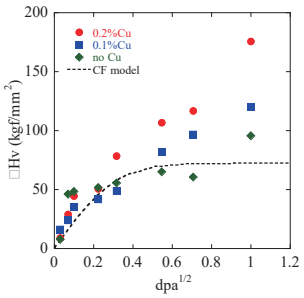

Figure 3 Irradiation hardening in 0, 0.1,and 0.2% Cu-0.8% Ni-1.4% Mn steels. Base hardening trend is consistent with newly developed CF hardening model.

Keywords: nuclear materials, radiation effects, positron annihilation
Takuya Yamamoto (Univ. California Santa Barbara)
Collaborators: Peter Wells, Yuan Wu, G. Robert Odette (UCSB), Takeshi Toyama, Yasuyoshi Nagai (Tohoku U.)
E-mail: yamataku@engineering.ucsb.edu

Crystal growth and study of rare-earth free scintillators

During two short visits to ICC-IMR together with colleagues from IMR we were focused on the search and selection of rare-earth free materials what can be used as effective scintillators and phosphors. Among variety of potential candidates divalent tungstates were selected as the most promising ones.

The high density crystals of Ca, Sr, Cd, Zn, Pb tungstates due to their high quantum yield, makes it possible to use them as phosphors and scintillators to detect both high-energy particles and low-energy radiation (medical tomography). The application of such crystals gives the possibility to decrease dramatically the production cost because of rare-earth elements absence in the crystal lattice. During many years my laboratory in General Physics Institute in Moscow, Russia, has been investigating such materials and developed single crystal growth technology by the Czochralski technique. At that time my team has succeeded to produce high quality $CaWO_4$ crystals up to 2 inch in size which were used at CRESST-II project (Europe).

Meanwhile among all divalent tungstates Cadmium tungstate shows the most interesting properties (Fig. 1) [1].

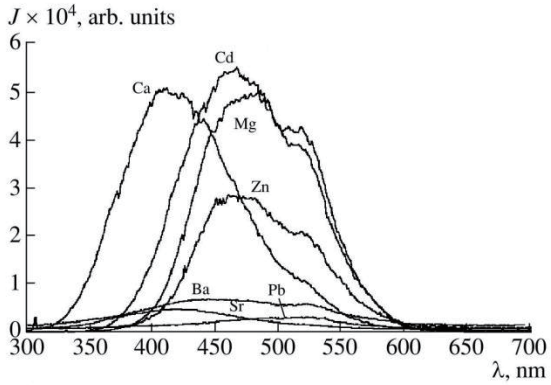

Fig. 1 Luminescence of divalent tungstates

This material has got good enough Light Yield (27000 ph/meV), short Decay Time (12 ns), high dencity (7.9 g/cm^2), and luminescence peak at 480-495 nm. However, scintillation properties of this material are very sensitive to the crystal growth conditions and after-growth treatment.

During my stay in IMR I was glad to join to the experiments for the crystal growth technology improvement with the final aim of growth of such crystals with the size up to 2 inch in diameter and stable set of parameters acceptable for the practical application. Fortunately, the students and researchers of the laboratory of Prof. Yoshikawa have got good experience in the crystal growth of different oxide scintillator crystals [2]. As a result even during my two short visits to ICC-IMR we succeeded together to grow crack-free $CdWO_4$ single crystal of 1.5 inch in diameter (Fig.2).

Fig. 2 As-grown CdWO4 single crystal

After treatment we plan to measure optical and scintillator properties of grown crystal, discuss the possible ways to improve them, and submit our results for journal and conferences. Also, we had few meetings about future experiments with the target to grow 2 inch CdWO4 crystal. Also, the possibilities to continue the search of other rare-earth free scintillator materials were discussed. Finally I would like to express my gratitude to ICC-IMR staff and all members of Yoshikawa laboratory for the invitation and help during my stay in Japan.

References

[1] A.A. Blistanov, B.I. Zadneprovskii, M.A. Ivanov, V.V. Kochurikhin
Crystallography Reports 50 (2005) 284-290

[2] A. Yoshikawa, V. Chani, M. Nikl
Acta Phys. Pol. A 125 (2013) 250-264

Keywords: Crystal growth, Scintillator
Full name: Vladimir Kochurikhin, General Physics Institute, Moscow, Russia
E-mail: kochurikhin@mail.ru
http://www.gpi.ru

Scintillation Properties of Nd^{3+}-Doped Lu_2O_3 Ceramics in the Visible and Near InfraRed Regions

Introductory. Nd:Lu_2O_3 ceramics were deeply studied for laser application and prepared in 2014 by the nonconventional spark plasma sintering (SPS) method. Radio-luminescence of the same ceramics was also observed, and several scintillation emission peaks were reported at 300–1200 nm under X-ray excitation. The near infrared emission within 900-1100 nm of the $^4F_{3/2} \rightarrow {}^4I_i$ (i = 11/2, 9/2) transitions of Nd^{3+} ions corresponding to the "human window" was successfully detected. Thus, Nd:Lu_2O_3 ceramics can be proposed as a candidate in medical applications including the dosimetry for radiation therapy. We propose to extend the topics in 2015 on rare earth-free scintillators as well as powder phosphors.

Nd^{3+}-doped Lu_2O_3 (Nd:Lu_2O_3) is a candidate for an infrared scintillator because (i) Lu_2O_3 has a high density of 9.5 g/cm^3 and a high atomic number of 67 and (ii) Nd^{3+}-doped materials emit in the infrared range and the emission lines from Nd^{3+} can be used in medical applications since human body has a transparency window between 600 and 1,100 nm. However, it is extremely difficult to fabricate Lu_2O_3 single crystals using conventional crystal growth methods because of the high melting point (2,510 °C). Using solid-state reactions, it is much easier to fabricate Lu_2O_3 into a ceramic structure. Therefore, Nd:Lu_2O_3 transparent ceramics were fabricated using a novel spark plasma sintering (SPS) method as can be seen in Fig. 1, [1]. This technique is comparatively simple and consumes less time than other methods such as vacuum hot pressing.

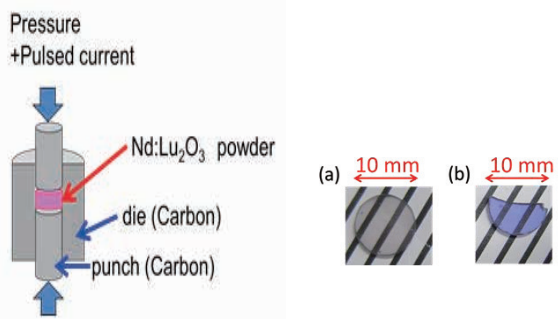

Fig. 1 Schematic view of SPS technique to fabricate Lu2O3 ceramics doped with 0.1 mol% (a) and 5.0 mol% (b) of Nd (after polishing).

Keywords: ceramic, oxide, luminescence,

Full Name: Georges Boulon,
ILM,UMR5306CNRS-UCBLyonVilleurbanne,France
georges.boulon@univ-lyon1.fr

The scintillation properties and transmittance spectra of the as-produced ceramics were studied in both the visible and the near infrared regions. Fig. 2 shows the radio-luminescence spectra measured in the range 800–1200 nm. Nd^{3+} emission lines were observed in the transparency window of human body. Thus, these ceramic materials could be a candidate for medical imaging applications [2].
The next analysis will be to develop a generic study on RE-free scintillators as well as powder phosphors and to develop new material conceptions in this field which have potential to provide commercially successful materials for several applications.

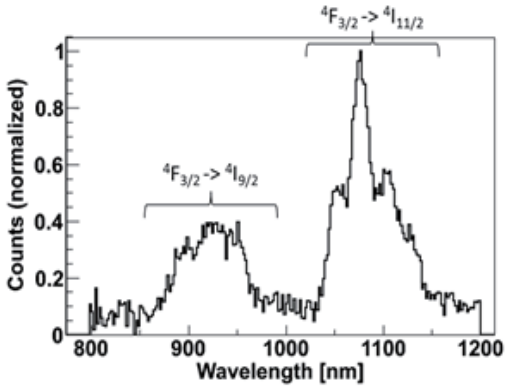

Fig. 2 X-ray-excited radio-luminescence of 0.5 mol% Nd:Lu_2O_3 in the near infrared region corresponding to the human window.

References

[1] G. Alombert-Goget, Y.Guyot, M.Guzik, G. Boulon, A.Ito, T. Goto, A. Yoshikawa, M. Kikuchi. Optical Materials 41 (2015) 3-11

[2] S.Kurosawa, L. An, A. Yamaji, A. Suzuki, Y. Yokota, K. Shirasaki, Y. Tomoo, A. Ito, T. Goto, G. Boulon, A. Yoshikawa, IEEE Transactions On Nuclear Science, vol. 61, p. 316-319 (2014)

Activity Report

Young Researcher Fellowships

FY 2014 Young Researcher Fellowships

No.	Name	Host	Proposed Research	Title	Affiliation	Term
14FS1	Andrea Impagnatiello	T. Shikama	Investigation of the Early Stage of the Precipitation in V-4Cr-4Ti Alloys by Position Annihilation Spectroscopy	Ph.D. Student	University of Manchester, UK	2014. 5.6-7.5
14FS2	Erin Kathleen Vehstedt	E. Saitoh	Spin-Charge Conversion Using Electronic Band Inversion Asymmetries	Postgraduate Research Student	University College London, UK	2014. 5.26-9.2
14FS3	Aditya Reza Haswendra	M. Niinomi	Investigation of Corrosion Property of Beta-Type Titanium Alloys in Simulated Body Fluid	Post-Graduate Student	Andalas University, Indonesia	2014.6.29-9.2
14FS4	Mingyue Ruan	H. Nojiri	High Magnetic-Field ESR Study on Spatially Confined Low-Dimensional Quantum Magnetic Materials	Ph.D. Student	Huazhong University of Science and Technology (HUST), China	2015.3.14-5.13

Electrical detection of non-equilibrium spin polarization with one part per million sensitivity based on the anomalous Hall effect

Precise room-temperature measurement and electrical control of spin polarization are a prerequisite for the integration of many novel spintronics devices into consumer electronics. We demonstrate that the principles of the well-known Hall effect can be extended to detect non-equilibrium spins at room temperature with one part per million sensitivity.[1,2]

The exotic phenomena which arise from non-equilibrium spin polarization or magnetization can occur due to tiny net moments,[3] which are beyond the sensitivity of existing measurement techniques. We propose a novel method of detecting such moments using a Hall voltage generated by non-equilibrium magnetization.

Fig. 1 shows a cartoon of our measurement setup. In the presence of a non-equilibrium magnetization, $\tilde{m}$, the spin-up and spin-down electrons are unequally populated in the normal metal and have spin Hall conductivities $\sigma_{SHE}\uparrow(\downarrow)$ depending on the spin-dependent chemical potentials $\mu\uparrow(\downarrow)$. When a charge current, j_c , is applied normal to $\tilde{m}$, a finite anomalous Hall-like voltage is generated. The effect was observed in both Au/YIG and CuIr/YIG bi-layered systems.

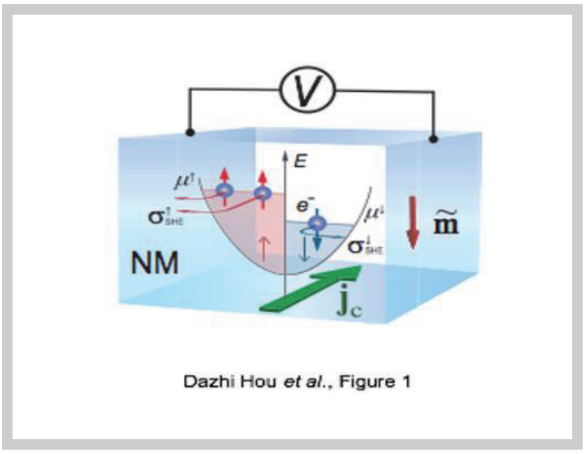

Fig.1 Anomalous Hall effect from non-equilibrium magnetization

This can be understood phenomenologically using a diffusion theory of the spin Hall effect. Microwave excitation is used to pump spins into the normal metal.

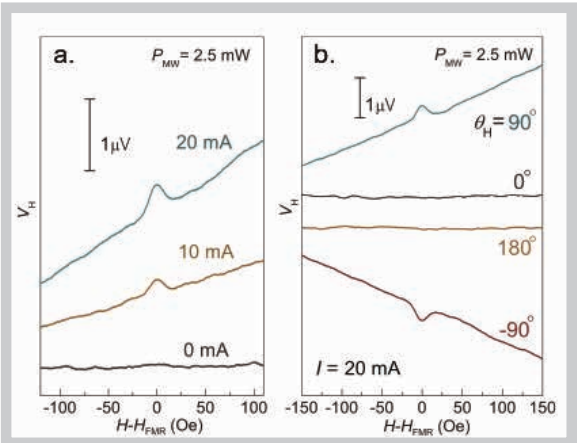

Fig.2 Non-equilibrium anomalous Hall effect in Au/YIG. (a) Hall signal dependence on applied current for P = 2.5 mW. (b) Angular symmetry of the Hall effect for j_c = 20 mA .

Spin accumulation in the metal layer acts as a non-equilibrium magnetization.[4] Under an applied electric field, Hall currents are produced via the spin-orbit interaction.

Fig. 2 shows the Hall signal measured at several currents for a 14 nm Au/YIG sample. Remarkably, this effect can be seen for power as low as 2.5 mW. In the low-power regime, thermal effects are negligible. Peak height scales linearly with current. Angular data (Fig. 2b) excludes an inverse spin Hall effect contribution.[5]

This technique provides a reliable method for non-invasive electrical detection of minute non-equilibrium magnetization in a broad range of materials. Furthermore, the energy derivative of the spin Hall angle, $\partial\Theta_{SHE}/\partial\varepsilon$, can be found from the anomalous Hall current, j_{AHE}, using other measurable quantities.[7] Thus the technique also provides access to a new parameter with which to characterize spin Hall materials.

Keywords: spintronic, magnetic insulator, spin excitation
Erin K. Vehstedt (Institute for Materials Research and London Centre for Nanotechnology/UCL)
E-mail: erin.vehstedt.14@ucl.ac.uk
http://saitoh.imr.tohoku.ac.jp

References

[1] E. H. Hall,. Phil. Mag. 10, 301 (1880)
[2] N. Nagaosa, et al, Rev. Mod. Phys. 82, 1539-1592 (2010)
[3] I. Zutic, et al., Rev. Mod. Phys. 76, 323-410 (2004)
[4] Y. Tserkovnyak, et al., Phys. Rev. Lett. 88, 117601 (2002)
[5] K. Ando, et al., Phys. Rev. B 78, 014413 (2008)
[6] S. Maekawa, et al., Spin Currents, OUP Oxford (2012)
[7] S. Lowitzer, et al., Phys. Rev. Lett. 106, 056601 (2011)

Keywords: spintronic, magnetic insulator, spin excitation

Erin K. Vehstedt (Institute for Materials Research and London Centre for Nanotechnology/UCL)
E-mail: erin.vehstedt.14@ucl.ac.uk
http://saitoh.imr.tohoku.ac.jp

Investigation of Corrosion Property of Beta-Type Titanium Alloys in Simulated Body Fluid

In order to obtain corrosion behavior of new β-type titanium alloy, Ti-29Nb-13Ta-4.6Zr (TNTZ) in Simulated Body Fluid (SBF), corrosion rate of TNTZ was investigated using a potensiostat test in Kubokko's solution (simulated body fuluid) as a model of a human body fluid. This would contribute to the advance of TNTZ usage as a prospective implants.

It has been reported that TNTZ alloy can have a wide range of mechanical properties by performing heat or thermo-mechanical treatments [1]. In order to know the potential of this alloy using as a new implant material, behavior of this alloy in body fluid is necessary to investigate.

Materials used in this study is TNTZ rods containing (in mass%) 31.5Nb, 11.6Ta, 4.7Zr, 0.03Fe, <0.02Al and bal. Kubokko's solution body fluid was prepared, according to related instruction [2] with temperature controlled in water bah at 37° and pH 7.4. Corrosion test was conducted using a potentiostat model controlled by a personal computer. After corrosion tests, TNTZ specimen surfaces were observed by OM and EDX.

Typical Tafel curves of TNTZ specimens (CP TNTZ 1, CP TNTZ 2, and CP TNTZ 3), which were obtained from potensiostat tests, are shown in Fig.1. The corrosion rate of TNTZ is also not too much different to that of Ti-6Al-4V ELI. Averaged corrosion rate of TNTZ in Kubokko's solution is 5.71×10^{-9} *mmy*$^{-1}$, while that of Ti-6Al-4V ELI is $4{,}49 \times 10^{-9}$ *mmy*$^{-1}$. This value is very much smaller than those of the conventional surgeon implant materials such as stainless steel SUS316L (2.13×10^{-3} mmy^{-1}) [3].

Pitting corrosion in TNTZ is found in some pattern-like such as elliptical and undercutting (Fig.2). EDX examination near pitting area shows that the content of oxygen in the corrosion area is much higher than that of the other area on the surface of TNTZ. This confirms the formation of pitting corrosion in the alloy.

The corrosion rate of TNTZ in this SBF fluid is almost same as that in the artificial saliva of Fuyusama Meyer: that is reported separetely by Gunawarman [4]. The high corrosion resistance of TNTZ is due to the formation of TiO_2 layer in the surface oxide layer of TNTZ in addition to the Nb, Zr and Ta oxides, whic acts as a transpassive layer. It can be said that the oxide layer formed on the TNTZ alloys is more stable, less soluble and thus more biocompatible than those of Ti-6Al-4V ELI. However, corrosion pitting attack is more potential in TNTZ as compared to Ti-6Al-4V ELI.

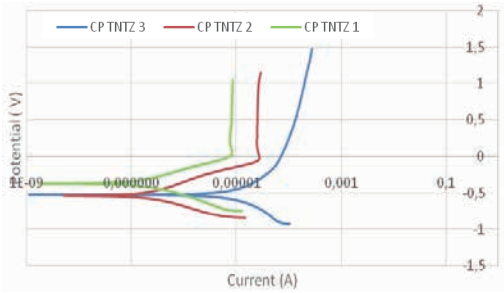

Fig. 1. Tafel plot TNTZ

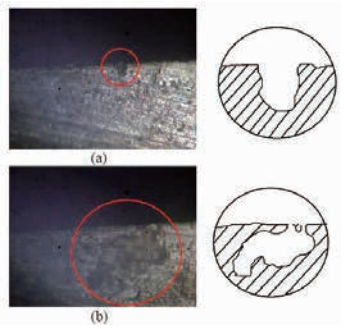

Fig.2 Pitting corrosion pattern-like on corroded TNTZ (a) Eliptical (b) Undercutting

Finally, I would like to thank very much to Prof. M. Niinomi, Asc. Prof. M. Nakai, Ass. Prof. K. CHO and all other Biomaterial Science Laboratory members for their help and corporation during this program. I aalso would like to thank IMR management for providing financial support as a young researcher at IMR. I would like to express special thanks to my supervisor Prof. Dr. Eng. Gunawarman, and co-supervisor Dr. Eng. Jon Affi at Andalas University, Indonesia.

During staying here, I could learn not only about this work, but also about Japanese culture. I have heard long time about Japanese spirit and discipline, and now I can prove it. It is better than what I previously imagined.

References

1. M . Niinomi, Mat. Mater. Trans. A 33A (2002) 477–486.
2. Ohtsuki, Chikara, How to prepare the simulated body fluid (SBF) and its related solutions.
3. M Talha, CK Behera, OP Sinhá, Journal of Chemical Pharmaceutical Research, 2012
4. Gunawarman, activity report as a visiting Professor in IMR, June-July 2014.

Keywords: Corrosion, Biomedical

1 Aditya Reza Haswendra (Biomaterial Science Laboratory)
E-mail: arkrezah@gmail.com

ICC-IMR FY2014
Activity Report

Edited by ICC-IMR Office
Published in February, 2018

Contact: International Collaboration Center,
Institute for Materials Research (ICC-IMR)
Tohoku University
2-1-1, Aoba-ku, Sendai, 980-8577, Japan
TEL&FAX: 81-22-215-2019
E-mail: icc-imr@imr.tohoku.ac.jp

Printing: HOKUTO Corporation

この冊子は「水なし印刷」により印刷しております。

環境にやさしい植物油インキ「VEGETABLE OIL INK」で印刷しております。